A TOPOGRAPHIC MAP OF FUNCTION ALONG THE AXIS OF STRIPES IN THE HINDBRAIN OF BEHAVING ZEBRAFISH

by Michael Robert Riley

The thesis/dissertation document has been electronically approved by the following individuals:

Joseph Fetcho (Chairperson)

Ronald Harris-Warrick (Minor Member)

David Deitcher (Minor Member)

Chris Schaffer (Minor Member)

A TOPOGRAPHIC MAP OF FUNCTION ALONG THE AXIS OF STRIPES IN THE HINDBRAIN OF BEHAVING ZEBRAFISH

A Thesis

Presented to the Faculty of the Graduate School

of Cornell University

In Partial Fulfillment of the Requirements for the Degree of

Master of Science

by

Michael Robert Riley

August 2010

ABSTRACT

The work described here represents an investigation into the functional organization of interneurons in the hindbrain of larval zebrafish. Four-day-old zebrafish are already freely swimming and can perform many of the adult motor behaviors, indicating that the networks are wired and functional. The hindbrain is, however, strikingly simple at this time. It is organized into a series of stripes, each with a particular neuronal type (based upon morphology and transmitter phenotype), with the neurons within a stripe arranged according to age and input resistance. Using calcium imaging and whole cell patch clamp, I tested the hypothesis that different populations of neurons along the axis of a stripe are recruited as a function of swimming speed. I found that younger, dorsal neurons in a stripe are recruited at lower swimming frequencies with older, more ventral neurons continuously recruited as swimming frequency increases. This illustrates a fundamental principle of organization in the hindbrain of larval zebrafish: that time of neuronal differentiation is a predictor of functional role. This functional organization has parallels with the pattern previously described for spinal cord, suggesting that it is a basic organizational principle that exists broadly in the nervous system. This simple organization, which is present at a time when the fish is already freely swimming, is likely masked later in life as neurons migrate and intersperse to form nuclei. The overall networks, however, are apparently established via a simple topographic, age-related patterning early in life, with neurons driving fast movements arising the earliest and increasingly slower ones layered on over time.

BIOGRAPHICAL SKETCH

Michael Riley is the oldest of two children. He grew up in Schenectady, NY and after graduating from high school he attended the State University of New York College at Plattsburgh. As an undergraduate at Plattsburgh, he studied biology and chemistry, which led him to develop a strong interest in the brain.

In June 2008, he pursued this interest by joining the doctoral program for Neurobiology and Behavior at Cornell University. In December 2008, he joined the lab of Dr. Joseph Fetcho and has remained in Dr. Fetcho's lab during his time at Cornell.

ACKNOWLEDGEMENTS

The author thanks Dr. Joseph R. Fetcho, Dr. Ronald M. Harris-Warrick, Dr. David L. Deitcher, and Dr. Chris Schaffer for comments on the manuscript. This work was supported by NIH Training Grant T32 GM007469 and NIH NS26539.

TABLE OF CONTENTS

BIOGRAPHICAL SKETCH…..……..iii

ACKNOWLEDGEMENTS……..iv

TABLE OF CONTENTS..……v

LIST OF FIGURES…….vii

CHAPTER ONE: INTRODUCTION..……..1

Organization of progenitor cells in vertebrate spinal cord……...1

V0 interneurons……..2

V1 interneurons……..2

V2 interneurons……..3

HB9 neurons……...3

V3 interneurons……..4

Functional organization of interneurons in spinal cord……4

Organizational parallels between spinal cord and hindbrain……6

Hindbrain networks are wired according to age……...7

Electrophysiological properties of alx neurons in hindbrain……8

CHAPTER TWO: A FUNCTIONAL ORGANIZATION OF ALX

NEURONS IN HINDBRAIN ACCORDING TO AGE……..9

Abstract……..9

Introduction……...10

Results……...11

A map of input resistance along the alx stripe……12

Recruitment of neurons along the alx stripe at different swimming speeds…15

Whole cell patch clamp recordings……...15

Calcium imaging……...21

Inhibition of alx neurons at faster swimming speeds…….25
Discussion……28
Methods……31

APPENDIX

A ground plan underlying the structural and functional patterning of neurons in the hindbrain of zebrafish…….35

REFERENCES…….65

LIST OF FIGURES

2.1 Input Resistances of alx neurons vary systematically along the axis of the alx stripe……...……..13

2.2 Recruitment patterns of alx neurons from whole cell recordings…….17

2.3 Relationship between swimming frequency at which each neuron is most active and cell body position…….…….19

2.4 Activation patterns of neurons within the medial glutamatergic stripe during swimming…….……..23

2.5 Inhibition of an alx neuron during fast swimming……26

CHAPTER 1

INTRODUCTION

The control of motor behaviors is an essential function for the survival of all animal species. Well-executed attacks against prey and coordinated, fast escapes allow individuals to survive in harsh natural environments. These behaviors are primarily governed by the hindbrain and spinal cord, where motor networks generate patterns of activity that coordinate appropriate muscle contractions for a particular type of movement. In order to generate those activity patterns, the networks must be wired precisely during their construction. Exactly how this phenomenon occurs, and what regulatory elements are responsible, has been a great challenge in the study of motor control. However, there is increasing evidence of simple principles of organization in the hindbrain and spinal cord early in the life of the animal that appear to govern the assembly of motor networks [1-10]. The work presented here will focus on the functional implications of such an orderly patterning in the hindbrain of larval zebrafish. I will first provide a brief overview of some of the known features of organization in both hindbrain and spinal cord.

Organization of progenitor cells in vertebrate spinal cord

It is well known that in the developing spinal cord, the gradients of two morphogens, Sonic hedgehog (Shh) and bone morphogenetic protein (BMP), generate multiple progenitor zones along the medial spinal cord [2, 11]. Neurons from dorsal progenitor zones are responsible for processing sensory information while ventral progenitor zones produce neurons that are part of motor networks [12]. The progenitor zones in ventral spinal cord (p0, p1, p2, pMN, and p3) each produce populations of neurons marked by particular transcription factors [1, 2, 13]. Neurons expressing these

transcription factors often share morphological and functional properties, and are discussed individually below.

V0 interneurons

Neurons from the p0 progenitor domain (termed V0 domain for differentiated neurons) express Evx1/2 and are primarily commissural [10, 14]. This particular domain is subdivided into two functional classes: excitatory neurons from $V0_V$ (ventral portion of V0) that express Evx1/2 and inhibitory neurons from $V0_D$ (dorsal portion of V0) that lack Evx1 expression [10, 14]. In *Dbx1* mutant mice lacking both inhibitory and excitatory V0 neurons, deficits in left-right motor coordination are observed [14]. However, *Evx* mutant mice lacking excitatory V0 neurons do not appear to exhibit this disruption of left-right coordination. Inhibitory V0 neurons from the $V0_D$ domain therefore appear to share a functional role in coordinating left-right alternation during walking.

V1 interneurons

V1 neurons derived from the p1 domain express Engrailed1 (En1), and have ipsilateral, ascending morphologies [15-18]. These neurons, when genetically ablated in transgenic mice, result in an increase in step-cycle period [19]. This is consistent with previous studies [17, 20-23] that suggest V1 interneurons might play a role in the coordination of ipsilateral flexor/extensor activity. Gosgnach et al. (2006) also report similar findings in adult mice that underwent allostatin-induced inactivation of En1 neurons [19].

In zebrafish, neurons from the p1 domain express Engrailed1, a homolog of the engrailed transcription factor in mice [15]. These neurons appear to have gross morphologies (ipsilateral, ascending), neurotransmitter phenotypes (glycinergic), and

functional roles (sensory gating and regulation of locomotor speed) that are shared across zebrafish, xenopus, and mouse spinal cord [15, 16, 19].

V2 interneurons

V2 interneurons come from the p2 progenitor domain and are further subdivided into the V2a and V2b classes [24]. In mice and chicks, V2a neurons express Chx10 and have primarily ipsilateral, descending morphologies and are functionally excitatory [2, 13, 25-28]. V2b neurons in mice and chicks express the GATA transcription factor(s) and are functionally inhibitory [24, 25, 27, 28]. Excitatory neurons that are derived from the p2/V2 domain in zebrafish spinal cord express the alx transcription factor (a homolog of Chx10) and VGlut2 transporter, and have ipsilateral, descending morphologies like those described in mice and chicks [7-9, 29, 30]. The similarity of transcription factor expression, neurotransmitter phenotype, and morphology of V2a spinal neurons across zebrafish, chick and mouse suggests partially conserved functional roles for these neurons throughout the evolutionary history of vertebrates. Those functional roles and the organization of V2a neurons will be discussed in greater detail in the following chapter.

HB9 neurons

HB9 interneurons express the HB9 transcription factor and come from the pMN progenitor domain, which also produces motor neurons [31]. These HB9 interneurons appear to have rhythmic capabilities [31-34], but their specific role in the central pattern generating system remains undefined.

V3 interneurons

Neurons derived from the p3/V3 domain are primarily contralaterally projecting and glutamatergic [35]. In neonatal mice, these neurons appear to exhibit properties that would suggest a role in central pattern generation such as moderate levels of spike frequency adaptation of a linear nature [35]. Disruption of synaptic transmission in these cells has been achieved through selective expression of the tetanus toxin light chain subunit (TeNT) in mice [36, 37]. These mice exhibited altered motor burst duration and step cycle period in both flexor and extensor nerves. Similarly, allostatin was used to temporally control the inactivation of V3 neurons in adult transgenic mice and also produced a deficit in consistency of motor burst duration [38]. This also affected symmetry of burst patterning on either side of the spinal cord, suggesting that V3 neurons play a role in coordinating motor output on the same side of spinal cord.

Functional organization of interneurons in spinal cord

Given the simple organization of progenitor domains in spinal cord and the clearly defined properties of neurons derived from each domain, it should not be surprising that this order has functional implications for spinal motor networks. Indeed, excitatory interneurons in larval zebrafish spinal cord are recruited according to a topographic map from ventral to dorsal as swimming speed increases [7, 9, 30]. This simple pattern of recruitment extends both within and across cell types, including multipolar commissural descending neurons (MCoDs) and circumferential ipsilateral descending neurons (CiDs). MCoDs are derived from V0 and express Evx1 (Shin-ichi Higashijima, personal communication) while CiDs are derived from V2 and express the alx transcription factor [30]. MCoDs, which are located in ventral spinal cord, therefore have the highest probability of firing at the slowest swimming frequencies

(roughly 15Hz). As swimming frequency increases, these MCoDs are less likely to fire because they are actively inhibited via glycinergic pathways. CiDs, which are active during fast escape movements and relatively greater swimming frequencies [7, 39], then are recruited into the motor network. Even within this neuronal subtype, the most ventral CiDs exhibit the most activity at the low end of higher frequency swimming (roughly 35Hz) and are inhibited as more dorsal CiDs are recruited during the greatest swimming speeds.

This type of organization is inherently different from the well-studied recruitment patterns of spinal motor neurons [40]. Motor neurons in spinal cord are recruited according to the size principle. During slow, less forceful movements, smaller motor units (with smaller neuronal somata and fewer muscles innervated) are active. As stronger, more forceful movements are generated, larger motor units (bigger somata and greater muscle innervations) begin to be recruited. The key difference between recruitment of these motor neurons and interneurons in zebrafish spinal cord is that, as more forceful movements are generated, the smaller motor units continue to stay active. Therefore, the total size of the active pool of motor neurons increases as movement strength increases. The active pool of interneurons, on the other hand, shifts from ventral to dorsal as movement strength increases in zebrafish.

Interestingly, this topographic pattern of recruitment of interneurons along the dorso-ventral axis of the spinal cord has yet another layer of organization. Those neurons that are located in the dorsal spinal cord and are active during fast swimming are also the first to differentiate [8]. Progressively younger neurons are then layered on over time in more ventral positions. Therefore, an age-related map of recruitment overlays the topographic map previously described: younger neurons drive relatively slow movements while older neurons are recruited to drive faster ones. This

organizational principle has revealed that time of neuronal differentiation is a predictor of later functional role.

These age-related patterns of recruitment also extend to inhibitory interneurons, which are organized in the reverse fashion. Older inhibitory neurons are located at roughly the same location in spinal cord as old excitatory neurons. Younger inhibitory neurons, however, are stacked dorsal to these. Consistent with the notion that age predicts function, young, dorsal inhibitory neurons are recruited at slower swimming speeds while older inhibitory neurons located ventral to these are recruited only as speed increases [7].

Organizational parallels between spinal cord and hindbrain

Given the similarities between spinal cord and hindbrain [41], it should not be surprising that many of the simple principles of organization in spinal cord extend to hindbrain as well [6]. First, the transcription factor code described in spinal cord appears to be conserved in zebrafish hindbrain. Even the relative order of those transcription factors appears to be conserved, except that the entire platform is topologically transformed from dorso-ventral in spinal cord to a more medio-lateral axis in hindbrain. Interestingly in hindbrain, neurons generated from individual progenitor zones and expressing certain transcription factors remain segregated in a stripe-like patterning (unlike spinal cord, where different neuronal subtypes are mixed following differentiation). These stripes, each of which contains neurons marked by a particular transcription factor, are also organized by age. The oldest neurons are located ventrally in a stripe, with progressively younger neurons stacked dorsally on top. Thus, age-related organization in hindbrain is inverted relative to spinal cord. Additionally, in each case where hindbrain neuronal populations expressing a

particular transcription factor have been identified, their gross morphology appears to mimic that of spinal cord neurons expressing the same transcription factor[6].

Hindbrain networks are wired according to age

The notion that neurons might be serially repeated across hindbrain segments has been suggested previously [4]. This study found that backfills of chick hindbrain neurons labeled longitudinal bands of cells that were organized along the medio-lateral axis. Indeed, the stripe-like patterning of hindbrain according to neurotransmitter, transcription factor, and morphological phenotype extends throughout all hindbrain rhombomeric segments [5, 6]. These findings suggest that functional neural circuits in hindbrain may be built using a simple wiring template whereby neurons with particular morphologies or neurotransmitters can be selected from individual stripes. Recent work has revealed how a single circuit, the Mauthner escape network in larval zebrafish, is built using neurons from different stripes (M. Koyama, in prep).

Such networks may also be built by selecting neurons from particular positions within a stripe. This would allow networks to wire according to age, such that older neurons will tend to wire to other old neurons and young with young. Experiments using a photoconvertable protein, Kaede, suggest that this is the case in the spinal cord and hindbrain of larval zebrafish [6]. In these studies, the relative age of neurons could be determined by the amount of green vs. red fluorescent protein expression. Neuropil regions of both hindbrain and spinal cord maintain age-related segregation. Stochastic labeling of alx neurons in zebrafish hindbrain has confirmed this age-related segregation of alx cell projections [6]. Alx cells located ventrally in the stripe have processes that tend to be located in older neuropil regions (medially and dorsally in hindbrain neuropil and medially in spinal cord neuropil). Similarly, alx cells located dorsally in the stripe have processes in ventral and lateral hindbrain neuropil and

lateral spinal cord neuropil. These findings have been extended to the single circuit level as well using whole cell patch clamp techniques (M. Koyama, in prep). All of the neurons in the well-studied Mauthner fast escape circuit are located ventrally in hindbrain at the bottom end of their particular stripe.

Electrophysiological properties of alx neurons in hindbrain

The recruitment patterns of spinal alx (CiD) neurons at least partially arise from a gradient of input resistance across the dorso-ventral extent of the spinal cord [7]. Young, ventral neurons have high input resistances and are easily excitable, while old, dorsal neurons have lower input resistances and therefore require stronger inputs to become active. Similarly, alx neurons in hindbrain have input resistances that are correlated with position and age [6]. Input resistance in these neurons increases with more dorsally located neurons in the stripe. Thus, in the work described here, I tested the hypothesis that young, dorsal alx neurons would be recruited at slow swimming speeds (when input strength is presumably small) and older, ventral alx neurons would be recruited only as swimming speed increased. This, in combination with recruitment studies in spinal cord [7-9, 30], would suggest that these simple principles of functional organization are present broadly in the nervous system and not simply an emergent property of spinal motor networks.

CHAPTER 2

A FUNCTIONAL ORGANIZATION OF ALX NEURONS IN HINDBRAIN ACCORDING TO AGE

Abstract

The organization of spinal neurons according to transcription factor expression, age, and morphology is present at a time when larval zebrafish are freely swimming, which requires that swimming networks be functional. Given the similarities of molecular, morphological, and age-related organization between spinal cord and hindbrain [6], we expected these features of functional order might exist in hindbrain at this time as well. Using the alx:GFP transgenic line of zebrafish, we investigated swimming-related recruitment patterns of alx neurons in hindbrain. Since time of differentiation, or neuronal age, is tightly correlated with dorsoventral position in hindbrain [6], we use position along the alx stripe (an easily quantifiable parameter in alx:GFP or alx:DsRed transgenic fish) as a marker of relative age. We found that neurons are systematically recruited along the axis of the alx stripe over a range of swimming speeds. Neurons near the dorsal edge of the alx stripe are active during slow swimming bouts while increasingly more ventral neurons become active at progressively faster swimming speeds. This organization appears to exist both within neurons that are expressing the alx transcription factor and in neurons that are near the alx stripe but are not alx+. These results suggest that neurons are organized in an orderly functional pattern broadly in the nervous system of the larval zebrafish and that this organization underlies coordinated, functional motor output at this time. We also show that alx neurons in the hindbrain are recruited in a manner that is very different from motor neurons, but similar to interneurons in spinal cord [9].

Introduction

Previous work has shown that hindbrain neurons are arranged in a stripe-like pattern, where individual stripes contain neurons with shared transcription factor identities and common morphological features [5, 6, 42]. Additionally, the age of these neurons, as well as their physiological properties, continuously vary along the axis of a stripe [6]. The organization of interneurons in hindbrain according to transcription factor, morphology, and age at a time when the fish is performing many of the adult behaviors suggests that functional neural networks might be built using a simple ground plan or template.

We investigated the functional organization of neurons along the axis of the alx stripe in 4 or 5 dpf larval zebrafish. Previous studies of zebrafish spinal networks at this age revealed a functional organization of interneurons according to age and position [7-9, 30]. Ventral alx neurons in spinal cord, which are relatively young, are recruited at slow frequencies of swimming. As swimming frequency increases, older alx neurons, located more dorsally, are recruited. This recruitment can at least partially be explained by the physiological properties of alx neurons. Ventral alx neurons in spinal cord have high input resistances and are easily excitable, while dorsal alx neurons have lower input resistances and are less excitable [7-9, 30]. Thus, a topographic map of recruitment according to age and input resistance exists in spinal cord.

In hindbrain, the age-related organization is topologically transformed such that later-differentiating, younger neurons are located more dorsally in a stripe while early-differentiating, older neurons are located more ventrally. As in spinal cord, the input resistance of neurons in hindbrain varies with age and position. In hindbrain, younger, dorsal neurons have relatively high input resistances while older, ventral neurons have relatively low input resistances [6]. Therefore, we hypothesized that

recruitment of alx neurons in hindbrain would follow a similar age-related, but topologically reversed, pattern from that in spinal cord.

Our data show that alx neurons are recruited from dorsal to ventral, as swimming frequency increases. This is supported both by whole cell patch clamp recordings as well as less invasive calcium imaging experiments. These results suggest that motor networks in the nervous system are organized broadly such that neurons' functional roles are determined by time of neuronal differentiation. They also suggest that recruitment of interneurons is inherently different from motor neuron recruitment. The active set of interneurons in hindbrain and spinal cord shifts at different swimming speeds whereas motor neurons increase the total size of the active pool of neurons.

Results

The presence of an orderly patterning of neurons by age, morphology, and input resistance raised the question of whether the neurons were incorporated into networks in an orderly way that varied systematically with position and therefore, age. To address this, we developed an approach to make targeted patch recordings from neurons deep in the brain *in vivo* in 4-5 dpf fish to allow us to explore their activity patterns. This technique involved removing the heart, yolk, swim bladder, and other organs of the ventral portion of the head. The notochord was then peeled back and removed, exposing the ventral surface of the hindbrain. When we patched from alx positive neurons in the caudal hindbrain in rhombomere 7, we found that some of the neurons were rhythmically active following light or electrical stimulation, which elicit slow and faster swimming respectively [7, 43]. To confirm that the neurons were indeed active during rhythmic swimming, we simultaneously recorded the motor pattern from an axial motor nerve to determine when swimming occurred and the

frequency of the bursts of activity, which is correlated with swimming speed [7]. Figure 2.1a shows that alx neurons fire action potentials in a rhythmic pattern that matches the swimming motor pattern recorded in the nerve, confirming their activation during swimming.

A map of input resistance along the alx stripe

We sought to confirm whether the input resistance of alx neurons varied systematically with their location in a stripe. Input resistance was measured by hyperpolarizing steps in patched neurons. Patch pipette solution included rhodamine dye that labeled patched neurons, allowing us to later measure their locations along the dorso-ventral axis of the stripe (see Methods). We sampled neurons from caudal hindbrain in R7-8 across the dorso-ventral extent of the alx stripe. Dorsal alx neurons consistently exhibited very high input resistances (often in the GΩ range) and had relatively long duration, small amplitude action potentials which would be expected of very young neurons. In general, neurons in roughly the top 30% of the stripe seemed to fire tonically and exhibited activity that was not correlated with swimming. Therefore, our results are comprised of data from neurons in the ventral 70% of the stripe that were clearly a part of swimming networks. Within this portion of the alx stripe, there was a significant correlation between input resistance and position as shown in Figure 2.1b (Pearson correlation: $P<0.01$). Input resistance was lowest at the bottom of the stripe and increased in more dorsal locations. While we did not include neurons in the top 30% of the stripe in our analyses, their input resistances were the greatest, consistent with the overall pattern. We also noticed that the resting potential correlated with position in that dorsal neurons tended to be more depolarized at rest and ventral neurons were more hyperpolarized (data not shown).

Figure 2.1 Input Resistances of alx neurons vary systematically along the axis of the alx stripe. **(a)** Whole cell recording of an alx:GFP expressing neuron in hindbrain segment 7 of a 5 dpf fish while simultaneously recording motor activity in a ventral root. Left: Example measurement of the normalized dorso-ventral position of a patched alx neuron (red) shown in cross-section. Cells were measured purely based on their position along the axis of the stripe (long white line), so that no medio-lateral positioning would be taken into account. This method was used to define the y-axis in **b**. White scale bar = 10um. Right: The patch recording from the alx cell on the left is shown below the simultaneous ventral root recording. The alx neuron shows rhythmic oscillations and fires during the swimming activity recorded in the ventral root. **(b)** Normalized position of cells within the alx stripe are plotted against their input resistance. Older, ventral cells tend to have low input resistances while younger, dorsal cells have greater input resistances.

a

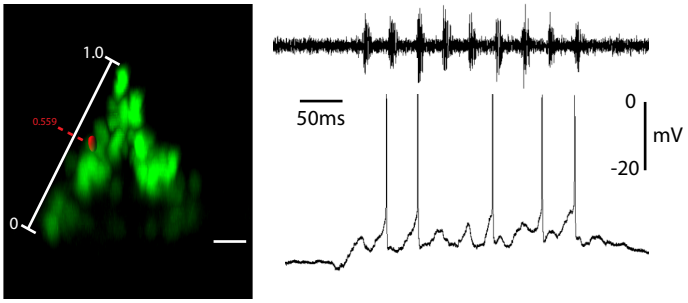

b

Input resistances of neurons along the alx stripe

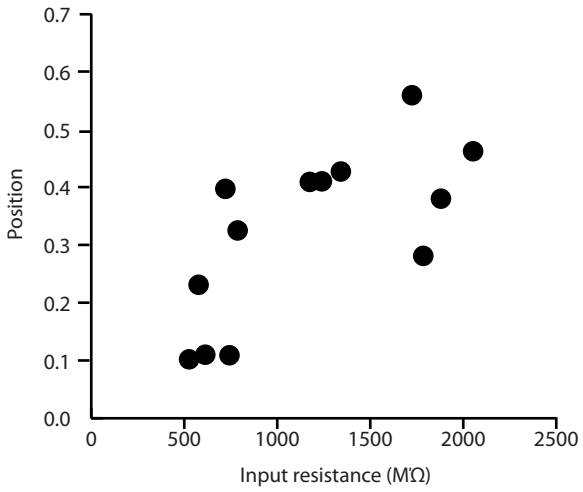

Recruitment of neurons along the alx stripe at different swimming speeds

Whole cell patch clamp recordings

We examined the activity of alx neurons (n = 12) over a range of swimming frequencies measured from the motor pattern recorded from an axial motor nerve. Neurons were grouped according to their normalized position along the dorso-ventral extent of the alx stripe [Ventral = .000-.200 (n = 5), Middle = .201-.400 (n = 4), Dorsal = .401-.600 (n =3)], and activity patterns were averaged (weighted mean) for neurons from each group. Many of the neurons from which we recorded showed rhythmic, sub threshold oscillations, but did not spike during the course of the experiment. Therefore, we estimated the amount of synaptic drive that neurons were receiving by measuring the maximum membrane potential reached during each burst cycle. The amount of depolarization was measured as the change from resting potential (referred to as "depolarization over baseline") as well as the change from the minimum membrane voltage in that cycle (referred to as "depolarization within cycle"). Both analyses of depolarization are shown as a function of swimming frequency (binned in 5Hz intervals) in Figure 2.2a,e,i and b,f,j. From these graphs, it is clear that dorsal neurons receive the greatest drive at swimming speeds near 25Hz and ventral neurons receive the greatest drive at roughly 55Hz.

In some experiments, we did find neurons that fired action potentials in time with bursts from motor nerves. For these neurons (n = 7), we calculated their firing probability at different swimming frequencies, again binned in 5Hz intervals, and averaged the results for the ventral, middle, and dorsal groups. The results, shown in Figure 2.2c,g,k, resemble the activity patterns from the depolarization analyses. We also examined the number of spikes per cycle of each of these neurons, depicted in Figure 2.2d,h,l. Dorsal neurons fired more action potentials per cycle at slower swimming speeds while ventral neurons tended to fire more spikes within a cycle only

during faster swimming.

We tested the significance of the relationship between position and each of the four measures of activity depicted in Figure 2.2 (depolarization over baseline, depolarization within cycle, firing probability, and spike number per cycle). The distribution of each of these parameters was examined for each cell, and the frequency of swimming at which the activity was greatest was plotted against cell position (Note: in 5 cases, the distribution contained outliers which were likely the result of a small sample size at that particular frequency. In these cases we plotted the maximum activity within the normal distribution). The results, shown in Figure 2.3, revealed significant ($p<0.05$) relationships between cell position and peak depolarization within cycle, peak firing probability, and peak number of spikes per cycle. Peak depolarization over baseline was not significantly correlated with cell body position ($p=0.1232$). However, this measure of activity is presumed to be the least accurate of those employed.

Figure 2.2 Recruitment patterns of alx neurons from whole cell recordings. Three groups are shown for dorsal **(a-d)**, middle **(e-h)**, and ventral **(i-l)** neurons. **(a-d)** Data from dorsal neurons (0.6< Stripe Position >0.4) are organized according to amount of depolarization over baseline at various frequencies **(a)**, amount of depolarization within cycle at various frequencies **(b)**, probability of firing at various frequencies **(c)**, and number of spikes per cycle at various frequencies **(d)**. Y-axis represents the change in membrane potential from rest in **(a)** and from the minimum voltage within that cycle in **(b)**. The number of cycles in which a cell fired an action potential is expressed as a percentage of the total number of cycles measured at that frequency in **(c)**. The number of spikes that were fired during each cycle for all dorsal neurons are shown as gray open circles (raw data) in **(d)** Closed black circles represent averages from data binned in 5Hz intervals. Plots are derived from 258 bouts from 3 cells in 3 larvae. **(e-h)** Data from middle neurons (0.4< Stripe Position >0.2) are arranged as in **a-d**. Plots are derived from 555 bouts from 4 cells in 4 larvae in **e-f**, and from 390 bouts from 2 cells in 2 larvae in **g-h**. **(i-l)** Data from ventral neurons (0.2< Stripe Position >0.0) are arranged as in **a-d**. Plots are derived from 357 bouts from 5 cells in 5 larvae in **i-j**, and from 43 bouts from 2 cells in 2 larvae in **k-l**. As swimming frequency increased, the active set of neurons shifted from dorsal alx neurons to ventral alx neurons.

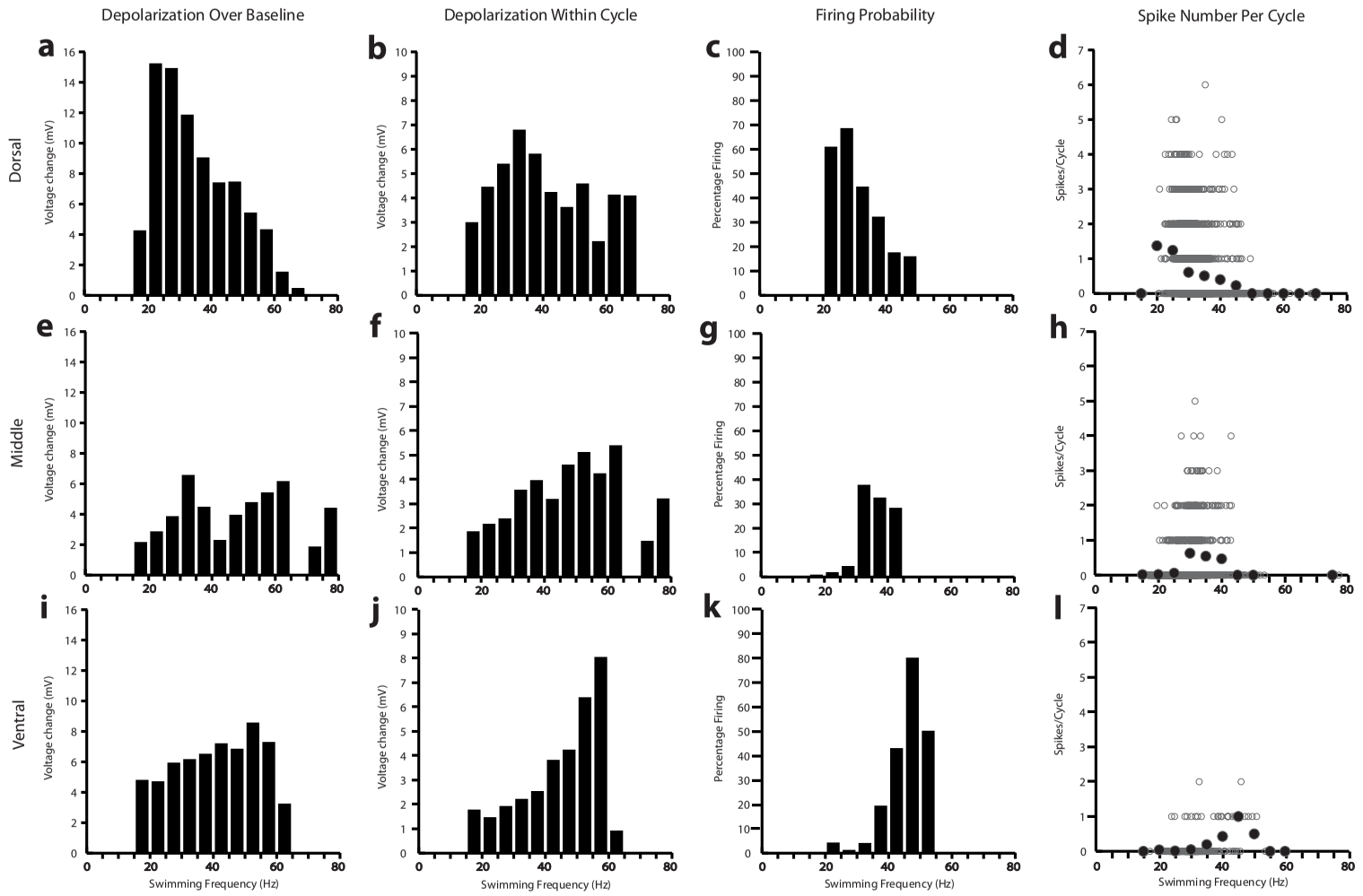
Depolarization Over Baseline
Depolarization Within Cycle
Firing Probability
Spike Number Per Cycle
Dorsal
Middle
Ventral
a
b
c
d
e
f
g
h
i
j
k
l
Voltage change (mV)
Percentage Firing
Spikes/Cycle
Swimming Frequency (Hz)

Figure 2.3 Relationship between swimming frequency at which each neuron is most active and cell body position. The swimming frequency at which each neuron showed the maximum amount of depolarization over baseline **(a)**, maximum amount of depolarization within cycle **(b)**, greatest firing probability **(c)**, and greatest number of spikes per cycle **(d)** is plotted against cell body position.

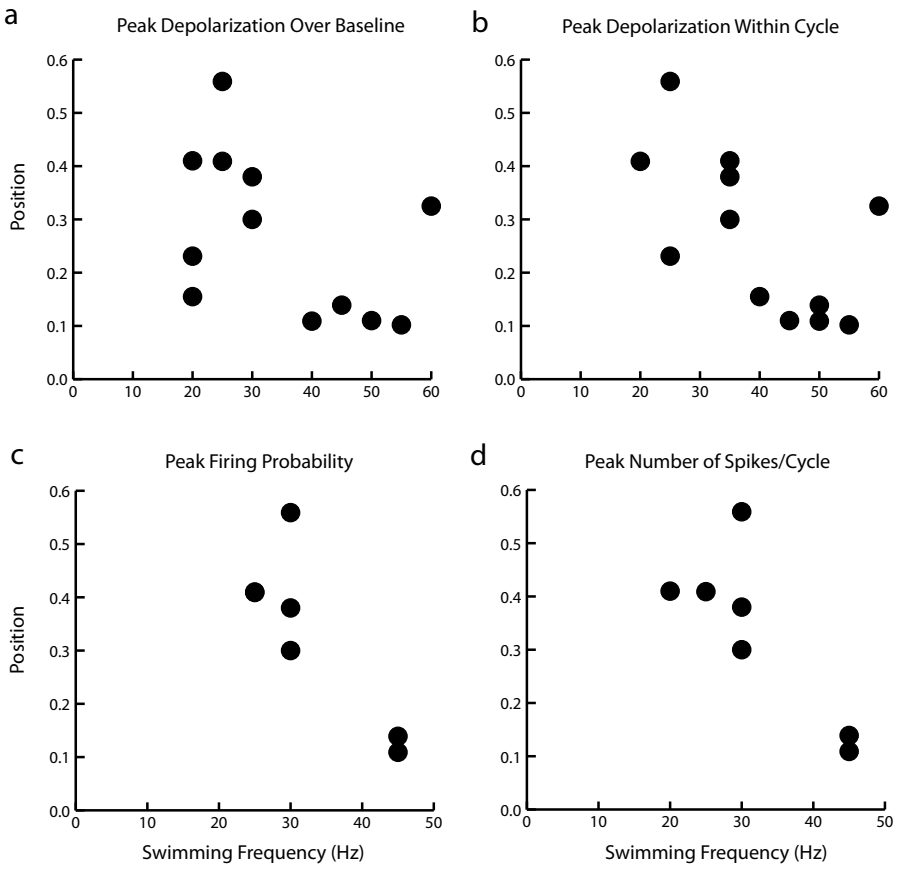
a
Peak Depolarization Over Baseline
b
Peak Depolarization Within Cycle
c
Peak Firing Probability
d
Peak Number of Spikes/Cycle
Position
Swimming Frequency (Hz)
0.0
0.1
0.2
0.3
0.4
0.5
0.6
0
10
20
30
40
50
60

Calcium Imaging

To rule out potential artifacts of patch clamp recordings, we also used less invasive calcium imaging to evaluate recruitment of alx neurons at different speeds of swimming. We labeled neurons in the alx stripe by electroporation of Oregon Green BAPTA-1 dextran (Invitrogen) into the alx:DsRed transgenic line. We then imaged activity patterns by monitoring dye fluorescence while simultaneously recording from ventral roots of the paralyzed fish to monitor the motor patterns. The approach is similar to one that was previously developed for spinal cord [7]. The major difference in our experiments, however, was that the calcium indicator was locally electroporated along the dorso-ventral axis of the alx stripe in R7-8. Short duration, low voltage (20ms, <5V) electroporations were performed at 4 dpf and imaging experiments were conducted the following day at 5dpf. At this time, fish were immobilized and prepared for simultaneous calcium imaging and ventral root recordings (see methods). Swimming episodes often occurred spontaneously, but we could more reliably elicit slower swimming by using flashes of blue light, or faster swimming by a brief electrical shock at the end of the tail. We determined the minimum recruitment frequency of individual neurons using an approach described in previous work [7, see Methods]. At the end of our experiments, we collected high quality image stacks through the hindbrain in the region of labeled neurons. This allowed us to later measure the position of the imaged cells along the dorso-ventral axis of the alx stripe.

Our experiments included multiple trials over a range of swimming speeds for individual neurons to determine their minimum recruitment frequency. Examples of calcium fluorescence traces from 3 alx neurons at different dorso-ventral positions are shown in Figure 2.4a. The top neuron exhibited a fluorescence increase in a bout with a peak frequency of 24 Hz, but not in one at 22 Hz, the middle neuron at 28Hz, but not 26Hz, and the bottom cell at 31 but not 29 Hz. Recruitment patterns and positions

were obtained for 29 neurons from 20 fish. Eleven of the neurons colocalized with alx:DsRed fluorescence and 18 did not, although the 18 non-alx neurons were in the general region of the alx stripe so their position along the stripe could be measured. Figure 2.4b shows a plot of the calculated minimum recruitment frequency versus position for the 3 cells in Figure 2.4a (green, yellow, and blue dots) superimposed on all of the neurons (gray dots). Figure 2.4c shows the minimum recruitment frequency both for neurons expressing the alx transcription factor (black dots) and for cells in the vicinity of the alx stripe (gray dots). Both populations of neurons showed a consistent pattern in which dorsal, younger cells were recruited at relatively slower swimming frequencies and increasingly more ventral neurons were recruited at increasingly faster swimming frequencies. The correlation between position and recruitment speed was significant ($p<0.05$) for all cases including: within the alx positive cells; within the non-alx positive neurons; and when both groups were pooled. The results reveal that neurons are recruited from dorsal to ventral along the axis of the alx stripe as the frequency of swimming increases. Therefore, there is a systematic relationship between position, age, and recruitment that maps onto the dorso-ventral axis of the alx stripe. Because this pattern was observed in non-alx neurons as well, it likely represents a broad patterning in hindbrain.

Figure 2.4 Activation patterns of neurons within the medial glutamatergic stripe during swimming. **(a)** Examples of calcium imaging from alx neurons at different locations in the stripe at different frequencies of swimming in 5 dpf fish. Left: Locations of the neurons along the stripe. Colored dots correspond to those on in plot in **b**. Right: Calcium responses of the neurons on the left in two example trials at swimming frequencies near those when the neurons are first recruited. For example, the top neuron does not respond in a trial with peak frequency of 22Hz, but does at 24Hz. (**b)** Plot of the minimum swimming frequency at which a neuron responds (measured as described in methods) versus the dorso-ventral location of the neuron. This plot includes both alx positive neurons and other non-alx positive neurons in the region of the alx stripe. Neurons from **a** are shown in color. **(c)** Similar to the plot in **b**, but with the alx neurons in black and the non-alx cells in the same area in gray. Both show a similar relationship between recruitment and position, with neurons recruited from the top of the stripe down as the frequency of swimming rises. White scale bars = 10 um for all images.

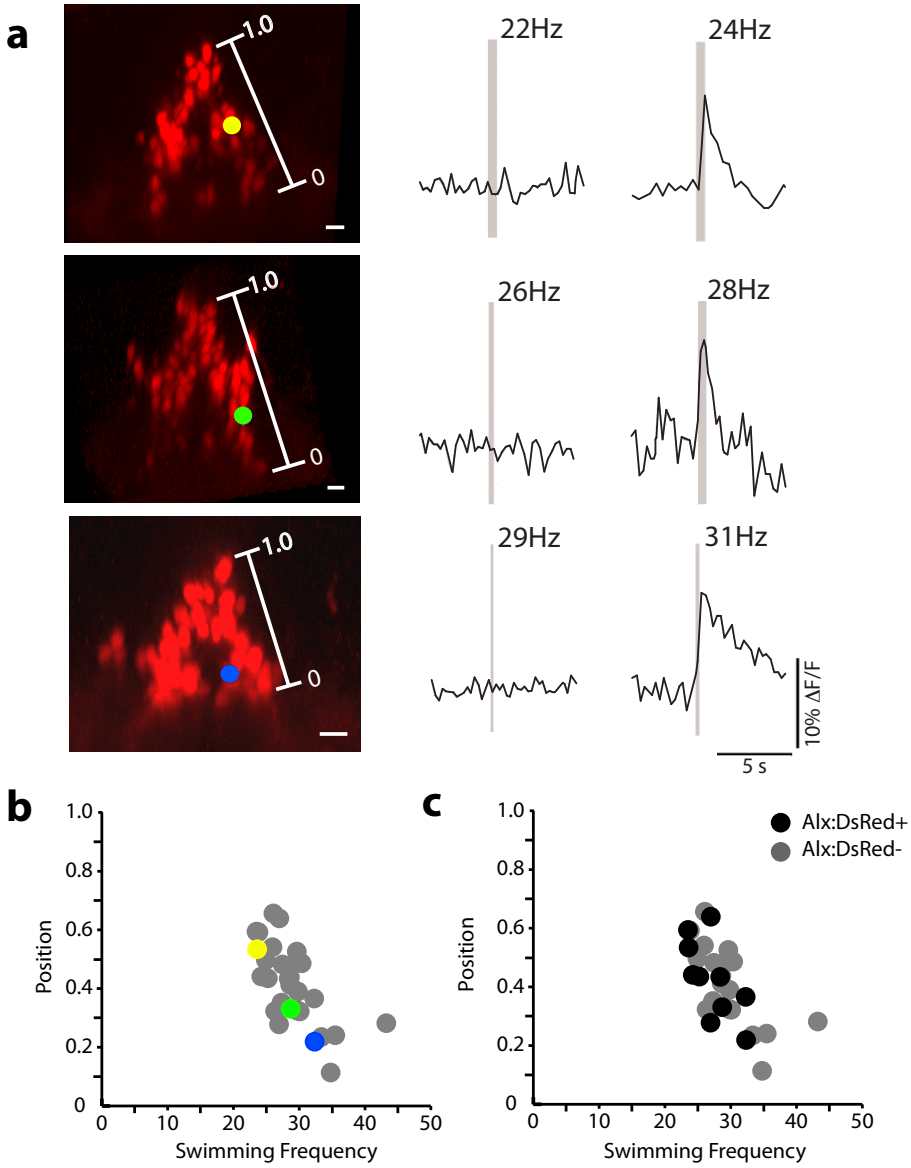
a
1.0
0
22Hz
24Hz
26Hz
28Hz
29Hz
31Hz
10% ΔF/F
5 s
b
Position
Swimming Frequency
c
Alx:DsRed+
Alx:DsRed-
Position
Swimming Frequency

Inhibition of alx neurons at faster swimming speeds

In our whole cell patch clamp recordings, we noticed that dorsal and mid dorso-ventrally positioned neurons (which tended to be most active during relatively slow to moderate swimming speeds) were less active during fast swimming. This coincides with a sharp decrease in firing probability of dorsal neurons at frequencies greater than roughly 35Hz and middle neurons at greater than roughly 45Hz (See Figure 2.2c,g,k). We investigated the possibility that these neurons were actively shut off during fast swimming by comparing their normal activity (no current injection) to their activity while injecting a steady, depolarizing current. In some neurons, artificially depolarizing the cell allowed us to see the endogenous, functionally inhibitory hyperpolarizing current during faster swimming frequencies. An example from a mid dorso-ventrally positioned neuron is shown in Figure 2.5. This active inhibition suggests that, as in spinal cord, neurons are not simply recruited at all swimming speeds at or above a certain value, but that the active set of neurons is continuously shifting as swimming speed changes.

Figure 2.5 Inhibition of an alx neuron during fast swimming. (**a)** Location of the patched alx neuron in **b** and **c** is shown in cross section. **(b-c)** Recordings of the alx neuron in **a** and a motor nerve in response to an electrical stimulus (asterisks) at two holding potentials. The response of the neuron at rest (+0pA) is shown in **b**, and the response of the neuron while injecting +10pA of current is shown in **c**. Holding the neuron at a more depolarized level reveals a hyperpolarizing current (gray arrow) at the beginning of the bout, when swimming frequency is greatest. Gray lines represent baseline membrane potential under each condition.

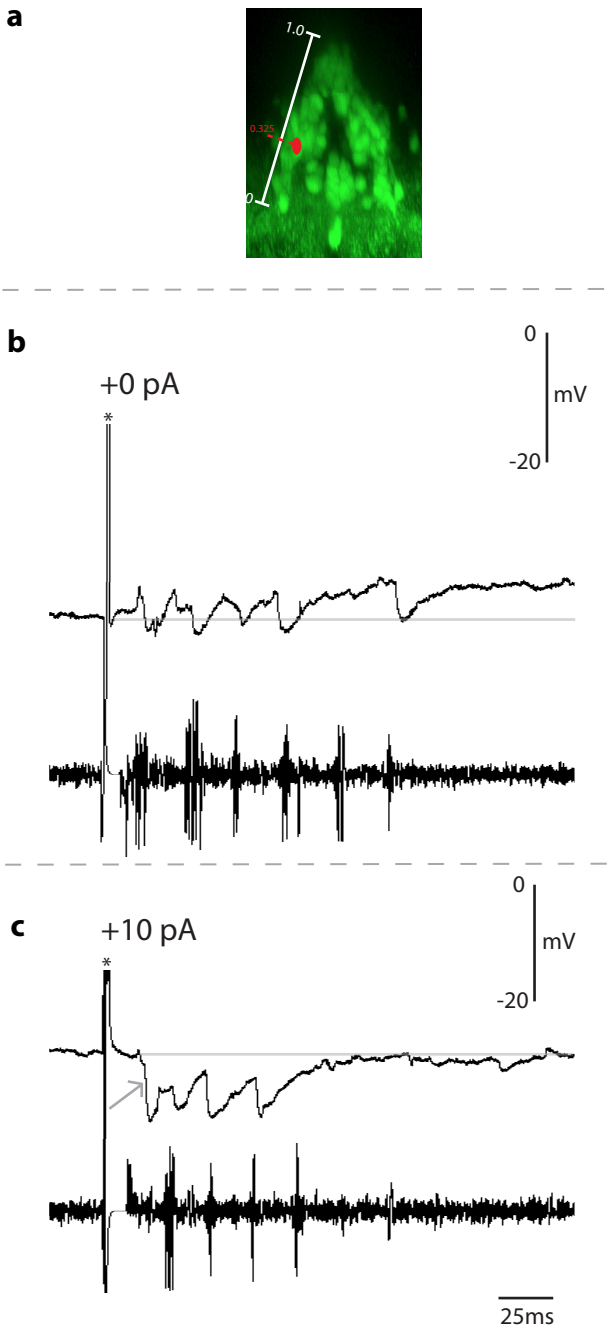
a
1.0
0.325
0
b
+0 pA
0
mV
-20
c
+10 pA
0
mV
-20
25ms

Discussion

These experiments reveal a simple pattern of functional organization in the brain of larval zebrafish. Neurons are recruited in a systematic fashion along the axis of the alx stripe in a manner that parallels activity patterns previously described in spinal cord [7-9, 30]. This patterning ultimately links time of neuronal differentiation to later functional role. Younger, dorsal neurons in a stripe are recruited at lower swimming frequencies with older, more ventral neurons continuously recruited as swimming frequency increases. Because the stripe-like patterning of hindbrain extends throughout all rhombomeres, it would not be surprising if the functional recruitment described here is part of a much broader underlying organization of motor networks.

The similarity between the activity patterns in hindbrain and spinal cord suggest a broad organizational principle that applies to the entire nervous system and is not simply an emergent property of spinal networks. Because this organization exists at a time when the motor networks controlling swimming, escape, eye and jaw movements are largely functional, it is likely that those circuits are built using a simple age (and position)-based template. The behavioral development of the animal supports this idea. The first neurons to develop are those driving the fastest movements, and the first swimming behaviors performed are fast escape responses. Slower swimming behaviors only develop later, presumably once the later-born neurons are incorporated into functional slow-swimming networks.

If networks controlling swimming at various speeds are wired using an age-related template, then we should expect age-related projection patterns to be present in the neuropil of both spinal cord and hindbrain. Kinkhabwala (2009) has examined the organization of neuropil using alx:Kaede and HuC:Kaede transgenic fish, and has shown a clear segregation of projections according to age [6]. Older neurons have processes located more dorsally in the neuropil and younger neurons have processes

located more ventrally. That author has also shown in other work using backfill experiments, that ventral, older neurons send their projections to other ventral neurons [6]. Similarly, dorsal, younger neurons send projections near other dorsal neurons. This suggests that neurons of similar age may connect with one another to form functional networks that drive swimming at a particular speed.

A system where somewhat different networks drive different frequencies of swimming appears likely and is supported by the active inhibition of some neurons in both spinal cord and hindbrain. We have shown that, in hindbrain, some alx neurons are shut off at speeds that exceed than their minimum frequency of recruitment. Mclean et al. (2008) observed a similar phenomenon in spinal cord [9]. This important finding has completely shifted our understanding of central pattern generating (CPG) networks. We now know that CPGs in both spinal cord and hindbrain can continuously shift between different sets of neurons as swimming speed changes. Importantly, this occurs in a manner that permits smooth transitions between speeds, whether accelerating or decelerating. An active shutting off of neurons in hindbrain in parallel with those in spinal cord suggests that neurons in this region are not simply providing drive to spinal CPG networks that then independently control the speed of swimming, but that they are an integral part of the functional CPG unit.

One important question regarding the functional recruitment of interneurons in hindbrain involves later migration of those neurons and the formation of nuclei in the adult brain. As neurons migrate, they may rewire in such a way that the patterns of recruitment observed in the larval stage are not conserved. This seems unlikely, however, as the cost of reorganizing the whole system while maintaining behavioral output would be great. A more likely scenario is that the basic principles of organization are set up early in the life of the animal and are conserved as the neurons migrate to form nuclei. This should include both recruitment order and patterns of

connectivity. While recruitment of most neurons has yet to be directly tracked into adulthood, functional segregation of older, primary and younger secondary motor neurons has been observed in both larval [7, 8] and adult [44] zebrafish. In both systems, older motor neurons are active only during fast swimming while younger motor neurons are recruited during slow swimming, just like the pattern for alx neurons. Alx type (CiD) neurons in adult goldfish have also been studied physiologically [39, 45, 46]. These neurons had primarily ipsilateral, descending morphologies and were recruited during relatively fast escape behaviors. Thus, the structure and function of these basic cell types appears to be conserved between adult and larval nervous systems.

In mice, Chx10 (an alx homolog) is expressed in a subset of interneurons, which, when genetically ablated, produces a deficit in fast locomotion [47]. This result suggests that the functional organization we have found in the larval zebrafish may also provide relevant information regarding the construction of motor systems in other higher vertebrates and tetrapods in particular. Similarly, the neurons driving the startle response in rats are among the earliest born [48, 49]. Molecular and morphological data also supports more direct parallels between zebrafish and mammalian systems. Studies of transcription factor patterning have found bands of many of the same transcription factors described in zebrafish that extend throughout the hindbrain of frogs, chicks, and mice [3, 50-55]. Clarke and Lumsden (1993) found that the projection patterns of neurons in the hindbrain of chicks were correlated with medio-lateral location of the cell body, suggesting that, like zebrafish, neurons in a particular hindbrain stripe in chicks share basic morphological features.

Taken together, all of these data point to a system in which vertebrate neural circuits responsible for motor (and probably other) behaviors are built using a simple, age-related template. In zebrafish, at least some of those circuits controlling swimming

appear to be composed of multiple networks that can be differentially activated during particular swimming behaviors. Interestingly, these components seem to be built using neurons that differentiated around the same time, located at particular locations in a continuum along the dorso-ventral axis from oldest to youngest. This age continuum has important functional implications: during slow swimming, the young component (dorsal in hindbrain, ventral in spinal cord) is active and as swimming frequency increases, the active component shifts ventrally in hindbrain and dorsally in spinal cord to include only the older cells. This represents a novel organization of motor networks that has yet to be described in higher vertebrate systems, but which likely forms the basic foundation of many neural circuits in the hindbrain of all vertebrates. A central challenge is now to determine whether this organization is retained into adulthood and, if so, how it is maintained as neurons migrate to form nuclei.

Methods

Fish care.

All experiments were performed on zebrafish (*Danio rerio*) between 3 and 5 dpf obtained from a laboratory stock of wild-type and transgenic adults. Larvae selected at 4 dpf were spontaneously swimming (between 96 and 106 hpf). Embryos and larvae were raised at 28.5°C in the same system as adults (Aquatic Ecosystems), but experiments were performed at room temperature (22 C). At these early ages, embryonic and larval fish are still nourished by the remnants of their yolk sac. All procedures conform to the National Institutes of Health guidelines regarding animal experimentation and were approved by Cornell University's Institutional Animal Care and Use Committee.

In vivo whole cell recordings in the hindbrain

Whole cell recordings were done in current clamp mode in 5dpf alx:GFP nacre transgenic larvae using modifications of methods described previously [7, 39, 43, 56]. Larvae were anesthetized using 3-aminobenzoic acid ethyl ester (MS-222, 0.02% in Hank's solution), paralyzed with alpha-bungarotoxin (1mg/ml in extracellular solution) and pinned twice through the notocord with tungsten pins to Sylgard in a small petri dish. The skin was removed from axial muscle between the pins for later ventral root recordings. The head was then rotated 90 degrees and pinned through the mouth. A small incision was made in the skin along a dorsal portion of the head for ease of patch electrode insertion. The dish, containing extracellular saline solution (134 mmol l^{-1},NaCl, 2.9 mmol l^{-1} KCl, 1.2 mmol l^{-1} MgCl2, 10mmol l^{-1} HEPES, 10 mmol l^{-1} glucose and 2.1 mmol l^{-1} CaCl2; adjusted to pH 7.8 with NaOH), was placed on a compound microscope (BX51WI; 641 Olympus, Melville, NY) and a glass microelectrode, filled with extracellular solution was placed over an intermyotomal cleft where the axial skin was removed. A MultiClamp 700A amplifier (Axon Instruments) was used to monitor extracellular signals in current clamp mode at a gain of 1000, with the low- and high-frequency cutoff set at 300 and 5000 Hz, respectively.

Patch-clamp electrodes were pulled from thin-walled glass capillaries to 10-20 MΩ resistances. To record from hindbrain neurons, the electrodes were filled with intracellular saline solution (ionic composition in mmol l-1: 125 K-gluconate, 2.5 MgCl2, 10 EGTA, 10 HEPES, 4 Na_2ATP; 6.25mg sulfur rhodamine-B, adjusted to pH 7.3 with KOH) and then gently advanced into the brain using motorized micromanipulators (Sutter Instrument Co.). Constant positive pressure (~20 mmHg) was applied to the micropipette using a pneumatic transducer (Bio-Tek Instruments Inc., Winooski, VT) until the tip of the electrode was brought within close proximity to a cell body. Cell bodies were visualized using differential interference contrast

(DIC) optics, and the alx postive identity of a cell was confirmed by briefly switching to an attenuated epifluorescent light source. A GΩ seal was then obtained either by equilibrating the micropipette to atmosphere or by applying gentle suction. A holding current of -65 mV was applied once the micropipette had become cell-attached and the membrane was penetrated with suction pulses. Whole cell current clamp recordings were made with a MultiClamp 700A amplifier (Axon Instruments) at a gain of 20 (Rf = 500mΩ) filtered at 30 kHz and digitized at 63 kHz.

Calcium imaging

Transgenic 4dpf alx:DsRed Casper fish (White et al., 2008) were first anesthetized using 3-aminobenzoic acid ethyl ester (MS-222, 0.02% in Hank's solution) and embedded in low melting point agarose (1.6% in Hank's solution, Sigma, St Louis, MO). A patch electrode (5-10MΩ resistance) was filled with 20% Oregon Green BAPTA-1 (10,000MW, Invitrogen/ Molecular Probes, Carlsbad, CA) and the indicator was electroporated along the dorsoventral axis of the alx stripe in caudal hindbrain by using a single cell Axoporator (-4V, 20ms duration square pulse, Axon Instruments). Larvae were then removed from the agarose, placed in a petri dish containing Hank's solution and stored in an incubator (28.5^{o}C) overnight.

The following day, we imaged the calcium indicator in hindbrain on a Zeiss LSM 510 inverted confocal microscope while recording from a ventral root using methods similar to those applied previously [7, 8]. The larva was oriented on its side, with the head at 90 degrees relative to the tail, and pinned in place. Once a stable root recording was in place, the hindbrain was imaged. A time series capturing OGB-1 and alx:DsRed transgenic fluorescence was acquired while simultaneously monitoring ventral root activity. Swimming often occurred spontaneously, but was also elicited by either flashes of blue light or a brief electrical stimulus applied to the end of the tail.

Following each experiment, we acquired high quality image stacks of the hindbrain for later reconstruction and cell positioning.

Analysis of calcium imaging and ventral root recordings was performed using custom written MatLab software. ROIs were selected to include single cells for measuring fluorescence intensity as an indicator of neuronal activity. The ventral root bursts were used to estimate swimming frequency during this activity, measured as the reciprocal of the period between the start of each successive burst. Due to the coarse temporal resolution of calcium imaging, we took a conservative approach to the measure of minimum swimming frequency at which a neuron was recruited, similar to McLean et al. (2007). For each swimming episode in which a neuron showed a calcium response (defined as >9% fluorescence increase over baseline), the fastest swimming frequency during that episode was recorded. We then averaged the lowest three of these values to estimate the minimum speed of recruitment, being sure to bracket the lowest frequency of recruitment by having episodes in which the neurons did not respond.

Image stacks were then reconstructed in 3D using Imaris software (Bitplane). Neurons that were active during the experiment were identified and isosurfaces were generated for each. The length of the left and right stripes (at the position of the cell body) were each measured three times and averaged. The distance from the top of the stripe to the center of the cell body was then measured three times and averaged. This distance along the dorsoventral axis of the stripe was then normalized for total stripe length at the position of the cell body.

APPENDIX

Title: A ground plan underlying the structural and functional patterning of neurons in the hindbrain of zebrafish.

ABBREVIATED TITLE: Hindbrain patterning

AUTHORS: Amina A. Kinkhabwala[1,2], Michael Riley[1], Minoru Koyama[1], Joost Monen[1], Chie Sato[3,4], Yukiko Kimura[3], Shin-ichi Higashijima[3,4] and Joseph R. Fetcho[1,*]

ADDRESSES: [1] Department of Neurobiology and Behavior, Cornell University, Ithaca, NY 14853, USA, [2] Princeton Neuroscience Institute, Princeton University, Princeton, NJ 08544, USA,
[3] National Institutes of Natural Sciences, Okazaki Institute for Integrative Bioscience, National Institute for Physiological Sciences, Okazaki, Aichi 444-8787, Japan,
[4]Department of Physiological Sciences, Graduate University for Advanced Studies (SOKENDAI), Okazaki, Aichi 444-8585, Japan

* Correspondence to: Joseph R. Fetcho, E-mail, jrf49@cornell.edu, Tel, 607 254-4341, Fax, 607 254-1303
FIGURES: 7
PAGES: 44
WORDS: Abstract (150); Introduction (607); Discussion (1587); Total: 12,531
KEYWORDS: Development; transcription factors; recruitment; locomotion; spinal cord; interneuron
ACKNOWLEDGMENTS: We thank David McLean for comments on the manuscript and Lindsay Heller for maintaining the many lines of fish. Supported by: NSF IGERT 0333366 (A.A.K.), NIH Training Grant T32 GM007469 (A.A.K. and M.R), the Ministry of Education, Science, Technology, Sports and Culture of Japan (S.H.), the Japan Society for the Promotion of Science (M.K.), and NIH NS26539 (J.R.F.).

ABSTRACT: The vertebrate hindbrain contains a variety of motor networks controlling movements of the eyes, jaw, head and body. We used transgenic labeling, calcium imaging, and electrophysiology to study the structural and functional organization of recently discovered neurotransmitter stripes that extend through the hindbrain. The stripes contain neurons with different gross morphologies that are marked by different transcription factors, and are arranged along the axis of a stripe by age, extent of axonal projection, and input resistance. Neurons within a single stripe are recruited systematically along the axis of the stripe according to swimming speed. The transmitter stripes thus reflect an underlying order that links the transcription factor expression patterns, age, morphology, and position of neurons within the stripes to their functional roles. We conclude that a simple structural and functional ground plan may form a foundation for the organization of the networks underlying the many behaviors produced by the hindbrain.

Introduction

The hindbrain and spinal cord are the principal motor output regions of the nervous system. They contain many specialized networks controlling the movements required for vision, respiration, mastication and locomotion in all vertebrates (Garcia-Campmany et al., 2010; Tumpel et al., 2009). Our recent work has focused on the question of whether there are principles of structural and functional organization within these vital regions of the nervous system (Bhatt et al., 2007; Liao and Fetcho, 2008; Liu and Fetcho, 1999; McLean et al., 2007; McLean and Fetcho, 2009; McLean et al., 2008; O'Malley et al., 1996).

Earlier studies showed that spinal networks develop via an orderly transcription factor code which serves to direct the differentiation of cell types with differing functional roles (Briscoe et al., 2000; Crone et al., 2008; Gosgnach et al., 2006; Lanuza et al., 2004; Pierani et al., 2001; Zhang et al., 2008). Our studies of spinal networks in zebrafish revealed functional patterns within populations of neurons marked by these transcription factors that link electrical properties and recruitment patterns to the position and age of the neurons (Higashijima et al., 2004b; Kimura et al., 2006; McLean et al., 2007; McLean and Fetcho, 2009; McLean et al., 2008). Some of the transcription factors expressed in spinal cord also mark neurons in hindbrain, raising the possibility of parallels between the structural and functional organization in the two regions (Cepeda-Nieto et al., 2005; Colombo et al., 2006; Moreno et al., 2005; Passini et al., 1998; Schubert et al., 2001; Storm et al., 2009; Thaeron et al., 2000).

Here we explore the structural and functional patterning of neurons in the hindbrain of zebrafish. The work was initially prompted by a striking patterning observed in earlier work in which we used *in situ* staining for markers of neurotransmitter phenotype to reveal putative glycinergic, GABAergic, and glutamatergic neurons in the hindbrain (Higashijima et al., 2004c). We found that neurons of the same transmitter phenotype were clustered together into stripes when viewed in cross sections, and that these extended as columns throughout much of the rostrocaudal axis of the hindbrain. This pattern was evident in larval fish at a time when they are freely swimming and most of the major adult behaviors driven by hindbrain -*e.g.* swimming, feeding, and eye movements - are functional. This organization raised the possibility that there might be a broad orderly patterning of neurons shared by all hindbrain networks.

We have now examined this by looking at the development, structure, and function of neurons in these neurotransmitter-defined stripes. We show that the transmitter stripes reflect an underlying order in the hindbrain that links the transcription factor expression patterns, age, morphology, and position of neurons within stripes to their activity patterns during behavior. The stripes contain neurons with shared morphological features that are ordered along the axis of a stripe both by age and by continuously varying structural and functional properties. Our evidence supports the view that this structural and functional topography forms a foundation for the development of the networks underlying the many behaviors produced by the hindbrain. This early order is obscured later in life when the nuclear organization of the adult vertebrate hindbrain is established (Wullimann et al., 1996). The

organization in hindbrain we describe has clear parallels with that in spinal cord (Briscoe et al., 2000; McLean et al., 2007; McLean and Fetcho, 2009; McLean et al., 2008), even though there are major differences in the two, given the specialized cranial sensory-motor networks located in the hindbrain. These parallels suggest that simple, shared organizational principles form a foundation for the construction of networks within those regions of the nervous system responsible for motor output.

Results:

Hindbrain transmitter stripes and transcription factor patterning:

The stripe patterning in the hindbrain was initially found by fluorescent *in situ* hybridization using the glycine transporter (glyt2) and the vesicular glutamate transporter (vglut2.1) as markers of transmitter phenotype (Higashijima et al., 2004c). The identification of these genes allowed us to produce BAC transgenic lines expressing green (GFP) and red (DsRed) fluorescent proteins driven by promoter regions of glyt2 and vglut2.1 (vglut2) respectively (Bae et al., 2009; McLean et al., 2007). We carefully examined the stripe pattern in more than 20 larval fish from each of these transgenic lines. The stripes were clearly evident in the hindbrain of dual transgenic lines (vglut:DsRed x glyt2:GFP), as shown in the example from a four days post-fertilization (dpf) fish in Figure 1 (N=16). In cross sections, these stripes were organized in an interleaved manner from medial to lateral on each side of the brain (Fig. 1A-C). The most medial stripe of neurons was glutamatergic and extended predominately dorsoventrally; the next more lateral labeled stripe was glycinergic and also extended dorsoventrally. This alternation between glutamatergic and glycinergic stripes continued to the lateral edge of hindbrain. While the stripe-like pattern was more evident in some hindbrain regions than others, it was found in all the hindbrain segments (rhombomeres) containing both glycinergic and glutamatergic interneurons (Rhombomeres 4 (R4) and 6-8 (R6-8) are shown in cross section in Figure 1B1-4). While the glycinergic and glutamatergic neurons were segregated from one another in this columnar pattern, there were other unlabeled neurons, both scattered within stripes and in large contiguous areas outside of the stripes that are probably neurons with other transmitter phenotypes (cholinergic and GABAergic for example) based upon prior in situ staining (Higashijima et al., 2004c). The stripe-like pattern of glycinergic and glutamatergic neurons was evident even after the fish have hatched and are engaging in the many behaviors that involve the hindbrain, such as swimming and escape, as well as jaw and eye movements, all necessary for survival.

Given prior work from other groups showing evidence for clustered expression of individual transcription factors in hindbrain (Cepeda-Nieto et al., 2005; Colombo et al., 2006; Moreno et al., 2005; Passini et al., 1998; Schubert et al., 2001; Storm et al., 2009; Thaeron et al., 2000), we next investigated the relationship between the transmitter stripes and transcription factor expression. We chose to focus on four transcription factors whose expression has been described previously within spinal cord (Colombo et al., 2006; Fjose et al., 1994; Higashijima et al., 2004b; Li et al., 2004; Pierani et al., 2001; Rachidi and Lopes, 2006). These included alx (called chx10 in mammals), dbx1b, engrailed-1 and barhl2. The locations, relative to transmitter stripes, of neurons expressing these transcription factors were examined by

crossing transgenic lines in which fluorescent protein was expressed in cells of a particular transmitter phenotype with lines expressing a different color protein in neurons of a specific transcription factor type. The transcription factor engrailed-1, for which we had no transgenic line, was studied by immunostaining for the protein in a glyt2:GFP transgenic line.

As Figure 2 shows, transcription factors were expressed in stripe-like patterns resembling the patterning of transmitter stripes. Neurons expressing the alx (chx10) transcription factor were clustered medially and extend dorsoventrally, like the neurotransmitter stripes located medially (figure 2A1; N=20). Cross sections in Figure 2A1-3 from a confocal image stack of an alx:GFP x vglut:DsRed transgenic fish imaged *in vivo* show that this medial cluster of alx neurons overlaps the medial glutamatergic stripe of neurons. Three-dimensional colocalization (see methods) of GFP and DsRed revealed that most, if not all, medial glutamatergic stripe neurons express the alx transcription factor (Figure 2A3, N=2 fish). Immunostaining for alx protein in the alx:GFP transgenic line confirmed that this line reliably marked the alx positive neurons in the hindbrain stripes (N=9; data not shown).

An example from a 4 dpf fish of immunostaining for engrailed-1 (en1) in the glyt2:GFP transgenic line is shown in cross section in panels B1-3 of Figure 2 (N=8; 4 at 5dpf and 4 at 54 hours post-fertilization(hpf)). Immunostaining for engrailed-1 was located in a stripe just lateral to the alx (medial glutamatergic) stripe and overlapping the medial glycinergic stripe (Figure 2B1-2). Colocalization indicated that most, if not all, of the neurons in this glycinergic stripe express engrailed-1 (Fig. 2B3; N=4).

Neurons labeled in the dbx1b:GFP transgenic line were clustered into a dorsoventrally oriented column of neurons located lateral to both the engrailed-1 and alx stripes (Fig. 2C1-3). Cross sections of the hindbrain from a dbx1b:GFP x vglut:DsRed transgenic fish shows that the cluster of dbx1b:GFP neurons overlaps with the glutamatergic stripe just lateral to the engrailed-1 stripe (Fig. 2C1-2). Dbx1b:GFP expression colocalized with both glutamatergic and non-glutamatergic neurons (Fig. 2C3; N=2). The glutamatergic dbx1b positive neurons were in the medial part of the dbx1b zone, whereas the more lateral region included the location of a glycinergic stripe, indicating that the dbx1b area encompassed at least a medial glutamatergic domain and, most likely, a more lateral, glycinergic one. Interneurons associated with dbx1 expression in spinal cord are known to be both glycinergic and glutamatergic with the two transmitter phenotypes arise from adjacent dorsoventral progenitor zones within the dbx domain (Pierani et al., 2001). Our observations indicate that a similar pattern occurs in hindbrain with a mediolateral segregation of the neurons by transmitter phenotype.

Neurons expressing the barhl2 transcription factor were located in a band at the lateral edge of the hindbrain (Fig. 2D1-3, N=10). This region of barhl2 neurons included some of the neurons within the lateral crescent-like stripe of glutamatergic neurons throughout hindbrain (Fig. 2D3; N=6), but not all of them. Colocalization indicated that, in some hindbrain regions, barhl2 marked the most lateral glutamatergic neurons in this crescent (Fig. 2D3), with non-barhl2 expressing cells located more medially within the crescent of glutamatergic neurons. This pattern changes rostrocaudally across hindbrain segments (rhombomeres); however, neurons in the

lateral region of the lateral glutamatergic crescent express barhl2 across all rhombomeres.

These data support the conclusion that transcription factor stripes lie in regular relationships with the neurotransmitter stripes (Fig. 2, far right panel). Neurons expressing particular transcription factors are clustered into bands that align with neurotransmitter stripes and, depending on the transcription factor, can be coextensive with a transmitter stripe (alx, engrailed-1), overlap multiple transmitter stripes (dbx1b), or overlap only a restricted, spatially segregated portion of a stripe (barhl2).

Because the transcription factors we studied are known members of the transcription factor code directing the differentiation of neurons in spinal cord (Briscoe et al., 2000), we examined how the distribution of cells expressing these transcription factors changes from spinal cord into the hindbrain by examining optical cross sections at different rostrocaudal locations within confocal image stacks acquired *in vivo*. Figure 2E shows the transition from spinal cord to hindbrain for two transcription factors (alx and barhl2), derived from dorsoventrally segregated spinal progenitor zones. In the spinal cord, shown in cross section in Figure 2E5, barhl2 neurons form a horizontal band (barhl2:GFP) dorsal to a band of alx neurons (alx:GFP), as in other species (Al-Mosawie et al., 2007; Alvarez et al., 2005; Briscoe et al., 2000; Rachidi and Lopes, 2006). Within the hindbrain, barhl2 neurons occupy a stripe lateral to the stripe of alx neurons, with both extending dorsoventrally (Fig. 2E1-3). There is thus a topological transformation from spinal cord to hindbrain in which the dorsoventral segregation within spinal cord gradually changes at its rostral end into a mediolateral segregation of transcription factor types in hindbrain (Fig. 2E1-5). The transformation is as if the neural patterning in spinal cord is split dorsally along the midline and opened like a clam shell to produce dorsoventrally oriented stripes in hindbrain, as opposed to mediolateral ones in spinal cord.

Morphology of neurons in the transmitter stripes.

We next examined the morphology of neurons within and across stripes to determine whether neurons within individual stripes were morphologically similar to one another and distinct from those within other transmitter stripes. By stochastic expression of membrane targeted protein mMCherry) under control of the glycine transporter promoter (via single-cell stage injections of glyt2:Gal4, UAS:mMCherry) in the glyt2-GFP transgenic line, we could randomly label isolated glycinergic neurons in red, map their location in a GFP labeled glycinergic stripe by imaging *in vivo*, and reconstruct the morphology of the neurons in three dimensions. We also did similar experiments labeling neurons located in the medial glutamatergic (alx/chx10) stripe by stochastically expressing either mMCherry or mGFP in single neurons in the alx:GFP and alx:DsRed transgenic lines, or Brainbow-1.1 in multiple neurons in the alx:GFP line (Livet et al., 2007).

Reconstructed neurons from these four stripes - the medial glutamatergic stripe and the three glycinergic stripes - are shown in dorsal view in Figure 3. All neurons were imaged at 5-6 dpf and reconstructed using Imaris (Bitplane) filament reconstruction software (see Methods). All 34 labeled medial glutamatergic stripe (alx) neurons (12 shown in the figure) imaged and reconstructed from hindbrain

rhombomeres 4-8 had ipsilaterally projecting axons (Fig. 3A). Despite differences in dorsoventral, mediolateral, and rostrocaudal positions of their cell bodies within this hindbrain stripe, all of the neurons had a descending axon, also characteristic of alx neurons within spinal cord (Kimura et al., 2006; Saueressig et al., 1999). All of these axons descended caudally as far as we imaged, often into spinal cord. While the alx neurons shared transmitter phenotype, stripe location, and a descending axon, they varied in other respects, including, most dramatically, some neurons that had an ascending axonal branch that was absent in others.

Figure 3 also shows three-dimensional reconstructions of neurons in the medial (engrailed-1, Fig. 3B), middle (putative dbx1b, Fig. 3C), and lateral (Fig. 3D) glycinergic stripes. For the medial and lateral glycinergic stripes, neurons were successfully labeled from rhombomeres 3 through 8 along the rostrocaudal axis of hindbrain. Those labeled in the middle glycine stripe were located within rhombomeres 6-8.

The medial glycinergic stripe neurons were predominately cells with ipsilateral and ascending axonal projections (13 of 15 neurons; Fig. 3B). Most of these axons were over 100 μm long (Fig. 3B) and projected as far, and typically farther, than rostral hindbrain. Of these 15 medial stripe neurons, the two unusual ones had in one case an ipsilateral descending axon and in the other a commissural descending axon. Both of these cells were positioned in caudal rhombomeres (R7-8).

All eight neurons labeled in the middle stripe had contralaterally extending axons with both ascending and descending branches, often of similar length (Fig. 3C). When one process was longer, the tendency was for it to be the ascending branch. These labeled cells in the middle stripe only projected within hindbrain.

Neurons in the third, lateral glycinergic stripe were unique in that they possessed what appeared, based upon morphology of the processes, to be both ipsilateral and contralateral axonal projections (Fig. 3D). This stripe possessed the largest variation in axonal trajectories. . The projections of most cells were confined to hindbrain, with some cells descending into spinal cord or ascending to more rostral brain regions. All seven neurons reconstructed had some combination of ipsilateral and contralateral axonal projections that distinguished them from those belonging to other stripes; however, there was variation in the presence and extent of ascending or descending projections on the two sides of the hindbrain.

Although these 63 reconstructed single cells from four of the transmitter stripes represent only a small fraction of the neurons in hindbrain, they reveal a general pattern consistent with the idea that these hindbrain stripes define broad morphological classes. Medial glutamatergic stripe neurons are ipsilaterally projecting cells with a descending axon, medial glycinergic stripe neurons are largely ipsilateral ascending cells, middle glycinergic stripe neurons have contralateral bifurcating axons, and lateral stripe glycinergic neurons have both ipsilaterally and contralaterally projecting axons. The transmitter stripes thus appear to contain neurons with different morphological features. This conclusion is also supported by a series of backfilling experiments designed to more specifically examine projection patterns within these transmitter stripes, as well as other work in which we explored the locations in the

stripes of neurons in the Mauthner escape network (M.Koyama, A. Kinkhabwala, J. Fetcho, in preparation).

Age-related patterning of alx neurons.

The previous sections focused on differences among the stripes and revealed that they differ with respect to neurotransmitter phenotype, transcription factor expression, and the morphological features of the neurons within them. We next examined the organization of neurons within a single stripe to determine if these neurons differed from one another. We chose to focus primarily on one stripe, the medial glutamatergic stripe of neurons expressing the alx transcription factor, for which we had the most morphological data, transgenic lines marking the stripe, and reason to think that at least some neurons in the stripe might be involved in swimming, like their counterparts in spinal cord.

We first used a transgenic line expressing the photoconvertible protein Kaede (alx:Kaede) in these neurons to investigate whether the neurons differed by age in an orderly manner along the axis of the stripe (Ando et al., 2002; Kimura et al., 2006). We photoconverted Kaede at different time points during development to generate fish with the earliest differentiating neurons labeled in red and the later differentiating cells in green (Fig. 4A, B). Intermediate aged neurons that expressed some Kaede before the color change and expressed new Kaede after the photoconversion contained both red and green protein and appeared yellow.

We found a broad and consistent pattern of age-related order in which the oldest neurons were ventrally positioned and the youngest ones populated more dorsal regions within the alx stripe. Figure 4C shows a lateral view of a photoconverted fish imaged *in vivo* from hindbrain to spinal cord, with cross sections at different locations shown below. The oldest neurons (red) are ventral to the youngest ones (exclusively green) across multiple hindbrain rhombomeres, with two exceptions in rhombomeres 6 and 8 (see asterisks). Rhombomere 6 contains two bands in which young alx neurons are ventrally positioned, and in rhombomere 8, one group of alx neurons lies medially, and thus outside of the stripe region.

To explore the age-related order of the alx stripe in more detail we photoconverted and imaged alx:Kaede fish at different times. Lateral views of these fish are shown as in Figure 4D1-3. In these examples, unlike 4C, we processed the images to show more clearly the location of the youngest, purely green neurons. The neurons shown in green here are ones that had no detectable red, and thus started expressing Kaede only after the photoconversion. The red ones are those that expressed at least some Kaede before the flash, and so contained at least some red (some also contained green, which was removed from them in these images; see Methods). The yellow in the images arises not from dual labeled red and green neurons, but from regions of overlap between red and green somata of different neurons within this lateral projection of image stacks. The green below the photoconverted

(red) neurons in the hindbrain region of Figure 4D1 is largely not from somata, but from the many processes of more dorsal, younger green somata that project into the ventral neuropil. .

In each case (Fig. 4D1-3), the vast majority of the youngest neurons (green) are dorsal to the older neurons located in red or yellow regions. The overall patterning in figure 4C-D was consistent across multiple fish photoconverted and imaged at different times (N=10, photoconverted between 24 hpf and 55 hpf and imaged between 33 hpf and 8 dpf). To explore the breadth of the age order in hindbrain, we also did a series of 22 additional color change experiments (not shown) using a transgenic line expressing Kaede under control of a general neuronal promoter (Huc). The line was typically crossed into transgenic lines labeling neurotransmitter and transcription factor stripes in green (glyt2, N=4; vglut, N=5; dbx1b, N=1; barhl2, N=6; Huc:Kaede alone N=6) to explore the location of the young and old neurons in the various stripes. These experiments supported the conclusion that the pattern in which the oldest neurons are located ventrally, with the younger ones stacked above them, is present broadly across multiple hindbrain stripes.

We also found an age related organization of the processes of the alx neurons in the neuropil. In the hindbrain, processes of older ventral neurons (red and yellow) are located dorsally in the neuropil, which lies just below the stripe of somata, while younger, dorsal neurons (green) have processes located more ventrally in the neuropil (Fig. 4E1). In contrast, in the spinal cord, which contains processes of alx neurons from both hindbrain and spinal cord, the older neuropil lies medial and dorsal to the younger neuropil (Fig 4F1). This neuropil patterning by age is present continuously from hindbrain to spinal cord, with the topological transformation described earlier for the neurons in the two regions accounting for correspondence between lateral (younger) neuropil in spinal cord and ventral (younger) neuropil in hindbrain.

To confirm this visually evident pattern, we quantified the intensities of red and green in cross sections using the approach described in the Methods section. An example for hindbrain is shown in Figure 4E2, and for spinal cord in Figure 4F2. Ventral regions in the hindbrain had little red neuropil, but significant amounts of green. In spinal cord, the quantification confirmed that the younger neuropil tended to be more lateral and ventral. We quantified this patterning in both spinal cord and in hindbrain within different rhombomeres (R4-8) for photoconversion/imaging at different times (photoconvert 2 dpf/image 3 dpf ; photoconvert 33 hpf/image 2 dpf in spinal cord; photoconvert 28 hpf/ image 5 dpf; and photoconvert 2 dpf/ image 4 dpf for R4-8 in hindbrain) and found the age-related order with the neuropil to be present in all 4 cases (N=1 for each). This age related patterning of projections raises the possibility that there might be age-related connectivity.

Structural and functional organization of neurons within the alx stripe in hindbrain.

In order to explore structural variation along the axis of a stripe, we examined the morphology of 19 alx neurons labeled stochastically with Brainbow-1.1 in different hindbrain rhombomeres at different positions along the axis of the stripe. We selected from these neurons those located in caudal hindbrain in rhombomeres six to eight, in which the overall dorsoventral extent of the stripe changes relatively little (those in R6 were in the middle of the rhombomere, a region not including the rostral and caudal edges where young neurons were located more ventrally, as shown in Figure 4C). The total axonal lengths of this subset of 10 cells were reconstructed in 3D (Fig. 5A, B) and measured using Imaris. These lengths were plotted against the locations of the neurons in the stripe (Fig. 5C), with the total stripe length normalized to one so that we could pool neurons from different fish. The axons of neurons in these relatively caudal segments projected into spinal cord, like the neuron shown in Figure 5A. A visual examination of the 19 neurons suggested that neurons located dorsally in the stripes had less extensive axonal lengths than those located more ventrally (the examples in Fig 5B are from different dorsoventral locations). This was confirmed in the plot of location versus axonal length for the quantified subset of 10 cells located in R6-8 in caudal hindbrain, which showed a significant ($p < .0001$) correlation between total axonal length and location (Fig. 5D). The total length of the axon (primary axon and branches) increased systematically, and nearly linearly, from dorsal to ventral along the stripe axis.

We next examined whether the input resistance of alx neurons varied systematically with their location in a stripe, as shown in Figure 5E. We initially used an exposed brain preparation to facilitate patch recording from ventral neurons in 5 dpf alx:GFP transgenic fish. Input resistance was measured by hyperpolarizing steps in patched neurons that were subsequently filled with dye, and their locations along the axis of the stripe were obtained after fixation and confocal imaging. We sampled neurons from the hindbrain in R7-8 across the dorsoventral extent of the alx stripe. Neurons positioned very dorsally had small amplitude, relatively long duration action potentials, a depolarized resting membrane potential, and very high input resistances, suggesting that they were very young, in accord with the Kaede photoconversion data (see above). We examined these dorsal neurons in a more intact preparation to determine whether their physiological properties were the result of damage. The results from this preparation were similar to those using the more exposed brain preparation, suggesting that the most dorsal neurons were immature, not damaged. In addition, we could elicit rhythmic motor activity during swimming in more ventral neurons in this preparation, but those above roughly 70% of the way up the stripe showed persistent activity that was not correlated with swimming. Consequently, we focused our input resistance and functional analysis on the ventral 70% of the stripe, which included older neurons that were clearly incorporated into networks.

Neurons with the lowest input resistance values were consistently located in the most ventral stripe regions at 5 dpf both in the preparations with massive exposure of the brain (black dots on Fig. 5E and those with reduced exposure (gray squares on Fig. 5E). There was a significant correlation between the position of a neuron along

the stripe axis and its input resistance within both preparations (Pearson correlation: $p<0.01$ for semi-intact preparation, $p<0.05$ for exposed brain preparation, $p<0.05$ for both together). The input resistance was lowest at the bottom of the stripe and increased in more dorsal locations in both cases, although the measurements from the more exposed preparation were more scattered (Fig. 5E). Although we illustrate only the neurons in relatively ventral regions, the very dorsal cells had even higher input resistances, consistent with the overall pattern.

The presence of an orderly pattern by age, morphology, and input resistance raised the question of whether the neurons were incorporated into networks in an orderly way that varied systematically with position and therefore, age. To address this, we developed an approach to do targeted patch recording from neurons deep in the brain *in vivo* in 4-6 dpf fish to allow us to explore their activity patterns. When we patched from alx positive neurons in the caudal hindbrain in rhombomere 7, we found that some of the neurons were rhythmically active following light or electrical stimulation, which elicit slow and faster swimming respectively (Masino and Fetcho, 2005; McLean et al., 2007). To confirm that the neurons were indeed active during rhythmic swimming, we simultaneously recorded the motor pattern from an axial motor nerve to determine when swimming occurred and the frequency of the bursts of activity, which is correlated with swimming speed (McLean et al., 2007). Figure 6A shows that the alx neurons fire action potentials in a rhythmic pattern that matches the swimming motor pattern recorded in the nerve, confirming their activation during swimming (see (Li et al., 2006) for a similar cell type in the hindbrain of tadpoles).

To explore the involvement of neurons at different dorsoventral locations in the alx stripe at different frequencies/speeds of swimming, we used calcium imaging. We labeled neurons in the alx stripe by electroporation of Oregon Green BAPTA-1 dextran (Invitrogen) into the alx:DsRed transgenic line. This allowed us to image activity non-invasively with the calcium indicator, while recording from ventral roots of the paralyzed fish to monitor the motor patterns. The approach is similar to one we previously applied in spinal cord (McLean et al., 2007). In this case, however, the dye was locally electroporated along the alx stripe region at 4 dpf and the next day the fish were immobilized and prepared for simultaneous calcium imaging and ventral root recordings (see methods). Although swimming often occurred spontaneously, a range of swimming speeds was induced by using flashes of light or by applying a brief electrical stimulus to the end of the tail. We determined the lowest swimming frequency at which a neuron was activated by using an approach described in previous work ((McLean et al., 2007); see Methods). We subsequently collected confocal image stacks through the hindbrain in the region of labeled neurons so that we could measure the position of the imaged cells relative to the axis of the stripe.

We collected many trials over a range of frequencies of swimming for each neuron to determine its minimum recruitment frequency. A few examples of calcium responses of neurons at different dorsoventral locations are shown in Figure 6B. In these examples, the top neuron exhibited a fluorescence increase in a bout with a peak frequency of 24 Hz, but not in one at 22 Hz, the middle neuron at 28Hz, but not 26Hz,

and the bottom cell at 31 but not 29 Hz. We obtained recruitment patterns and positions for 29 neurons from 20 fish. Eleven of the neurons expressed the alx transcription factor and 18 did not, although the 18 non-alx neurons were in the general region of the alx stripe so their position along the stripe could be measured. Figure 6C shows a plot of minimum recruitment frequency versus location for the cells in the color-coded examples shown in figure 6B superimposed on all of the neurons. Figure 6D shows the recruitment patterns both for neurons expressing the alx transcription factor (black) and for cells in the vicinity of the alx stripe (gray). Both alx and non-alx neurons showed a consistent pattern, in which more dorsal, younger cells were recruited at the lowest swimming frequencies and increasingly more ventral neurons were recruited at increasingly higher swimming frequencies. The correlations between location and recruitment were significant ($p<0.05$) for all cases including: within the alx positive cells; within the non-alx positive neurons; and when both were pooled. The neurons are recruited from dorsal to ventral along the axis of the stripe as the frequency of swimming increases, indicating a systematic relationship between position, age, and recruitment that maps onto the axis of the alx stripe and extends to other non-alx neurons as well.

Discussion:

Our experiments reveal that the striking organization into transmitter stripes in hindbrain reflects a broad patterning of neurons by cell type, morphology, cellular properties, and activity patterns that is summarized in Figure 7. The key elements of the patterning are: 1) an overlap between transcription factor expression patterns and the stripe-like organization, with some transcription factors such as alx (chx10) directly corresponding with transmitter stripes and others overlapping multiple stripes or portions of stripes; 2) the presence of cells with similar gross morphological features within each stripe: ipsilaterally projecting neurons with primarily descending axons in the most medial glutamatergic stripe, ipsilaterally projecting neurons with predominantly ascending axons in the most medial glycinergic stripe, contralaterally projecting neurons in the middle glycinergic stripe and commissural neurons with both ipsilateral and contralateral projections in the most lateral glycinergic stripe; 3) within a stripe, the neurons are arranged by time of differentiation with the oldest cells most ventral and the younger ones more dorsal; 4) cellular features such as total projection length and input resistance vary systematically with stripe position, with the lowest input resistances and most extensive axons in the ventral, oldest neurons and higher input resistances and shorter axonal lengths in the younger cells; 5) the neurons over at least 60-70% of a stripe are incorporated into circuits at this age, as we might expect because the fish is freely swimming over a range of frequencies, like adult animals; and 6) the neurons active during swimming are recruited systematically according to swimming frequency along the axis of the stripe, from younger dorsal neurons to older ventral ones as the swimming frequency increases. These observations indicate that the hindbrain is constructed in an orderly manner from a series of cell types with continuously varying structural and functional properties based upon age. These cell types are incorporated into networks to produce a broad range of movement frequencies and speeds.

The fish we studied are freely swimming larvae with functional motor networks for swimming, escape, jaw, and eye movements, all located in a hindbrain with a strikingly regular organization. The transcription factor and transmitter stripes both extend throughout the hindbrain, across the well-studied rhombomeres (Hanneman et al., 1988; Wilkinson et al., 1989), and through regions containing many different networks. The implication is that the many neural circuits in hindbrain are built via a common ground plan with a core set of neuronal types from which cells are drawn based upon their age to fulfill particular roles in network function.

The pattern observed here has obvious parallels to the patterning we have described in spinal cord, where there is an age and position related order of cellular properties and recruitment within different neuronal classes marked by particular transcription factors (McLean et al., 2007; McLean and Fetcho, 2009; McLean et al., 2008). These parallels, evident in our visualization of the continuous transformation of the transcription factor patterning in spinal cord into and within hindbrain, are consistent with the idea that much the same ground plan for networks extends throughout all of those regions of the nervous system that contain the networks providing motor output. The morphological features characteristic of cell types marked by particular transcription factors in spinal cord is conserved in hindbrain, with for example, alx neurons being glutamatergic with descending ipsilateral axons and engrailed1 neurons being glycinergic with primary ipsilateral ascending axons (Higashijima et al., 2004b; Kimura et al., 2006). In hindbrain, the transcription factor regions are expanded in size relative to spinal cord and the motor output is diversified to control a variety of motor functions in the head. This expansion of the number of cells in each category and their orderly alignment into extended stripes makes the patterning more evident and easier to study systematically in the hindbrain.

Some of the order evident at the larval stage is probably a consequence of the relative youth of the animals, with older more ventral neurons being more elaborate than the younger more dorsal ones, partly because of the differences in the time since they first differentiated. The neurons are stacked in order with the youngest at the dorsal ventricular zone and increasingly older ones ventral to them. Importantly, however, there are functional hindbrain networks at this time because the animals are behaving, and must behave to survive. Both the hindbrain networks and the behavior of the animal are therefore built upon the foundation of this patterning.

One key question, however, is whether this pattern simply represents a way of quickly constructing a functional motor system that is later rebuilt as the animal grows. A wholesale reorganization of the networks with further development seems unlikely, because the patterns of motor output in larvae parallel those in adults (e.g. the alternation and rostrocaudal delays characteristic of swimming are present throughout life (Fetcho and Svoboda, 1993; Liu and Westerfield, 1988; Masino and Fetcho, 2005)). A reconstruction of the networks would mean dispensing with a motor circuitry that already worked. The more likely possibility is that the essentials of the larval pattern of network organization and recruitment are retained even as the neurons disperse to reorganize into nuclei. If so, we would predict that if we could track neurons as the brain differentiated further, the recruitment order and the basic patterns of connectivity established early would be retained later in life.

Even though most neurons have not yet been tracked into adulthood to explore their functional roles over time, there is evidence for conservation of early patterns of recruitment and connectivity into adults in both spinal cord and hindbrain. In the spinal cord of larvae, the recruitment order of motoneurons is related to position and age, with early differentiating, so called primary motoneurons, recruited in the fastest movements and later arising secondary ones involved in slower movements (McLean et al., 2007; McLean and Fetcho, 2009). Physiological studies show that the primary motoneurons remain involved in faster movements than secondaries, even into adulthood (Liu and Westerfield, 1988). The recruitment patterns of interneurons are more difficult to assess, but other work identifying CiD (alx) type neurons in adult goldfish revealed a cell type with a morphology much like the early differentiating CiD interneurons that are involved in the fastest movements in larval zebrafish. This cell type in adult goldfish, like the one in larval zebrafish, is activated during escapes, suggesting a conservation of recruitment pattern into adulthood (Fetcho, 1992; Fetcho and Faber, 1988;Bhatt et al. 2007).

In addition, we have mapped the components of the hindbrain network of the Mauthner cell, which mediates the escape behavior, onto the stripe arrangement in larval zebrafish (M. Koyama, A. Kinkhabwala, J. Fetcho in preparation). The morphology of the neurons and pattern of connectivity of the larval escape network is nearly identical to the network that exists in the adult hindbrain of the closely related goldfish, suggesting that network connectivity patterns established early are retained later, even as the gross morphology of the brain and the distribution of neurons changes with growth (Faber et al., 1989). All of this evidence points to a conservation of at least some features of connectivity and orderly functional properties established in larvae, even as the stripe-like arrangement is obscured as neurons redistribute during the further growth of the brain.

Another major issue is whether the patterning evident in the hindbrain of zebrafish extends to other vertebrates. Studies of transcription factor staining, neuronal morphologies, and functional organization in other aquatic vertebrates, chicks, and mammals suggest that the organization in the hindbrain of zebrafish extends broadly among vertebrates. Longitudinal bands of some of the same transcription factors we studied extend through the hindbrain of frogs, chicks, and mice, and their locations relative to the midline parallel the patterns in zebrafish (Cepeda-Nieto et al., 2005; Colombo et al., 2006; Moreno et al., 2005; Passini et al., 1998; Schubert et al., 2001; Storm et al., 2009; Thaeron et al., 2000). Morphological data from backfilling studies in chicks indicates that neurons with different morphological features occupy systematic locations relative to the midline (Clarke and Lumsden, 1993), consistent with the orderly mediolateral disposition of the stripes and cell types we found in zebrafish.

The relationships between time of differentiation and functional roles are harder to establish in other species, and so have not been well studied. Nonetheless, there is evidence from other animals that is in accord with the zebrafish pattern. Those hindbrain neurons driving the startle response in mammals, which is their fastest motor response, are also the earliest born neurons, consistent with the relationship between age and function we found (Altman and Bayer, 1980; Lingenhohl

and Friauf, 1994). Even in humans, the fast startle response is the first motor response evident in utero (de Vries et al., 1982), as it is in the eggs of zebrafish, suggesting that the fastest movements are driven by the oldest neurons across vertebrates.

In summary, the striking order we found in the hindbrain of zebrafish probably extends to vertebrates more broadly. The structural and functional organization of hindbrain has some similarities to the patterning in spinal cord, suggesting that both hindbrain and spinal cord are built via a simple shared ground plan. While there are undoubtedly changes with growth, nervous system plasticity, and divergence in the networks for specific tasks, the basic features of structural and functional organization that we describe may lie at the foundation of the construction of the many sensory-motor circuits throughout the hindbrain and spinal cord. The challenge now is to understand how many different networks are constructed from this basic ground plan and how the early pattern is reorganized as the brain continues to differentiate into its adult form.

Methods:

Fish care. All experiments were performed on zebrafish (*Danio rerio*) between 1 and 8 dpf obtained from a laboratory stock of wild-type and transgenic adults. Embryos at 2 dpf were selected while still in their egg casing [between 48 and 54 hpf (hours postfertilization)]. Larvae selected at 4 dpf were spontaneously swimming (between 96 and 106 hpf). Embryos and larvae were raised at 28.5°C in the same system as adults (Aquatic Ecosystems), but experiments were performed at room temperature (~22 C). At these early ages, embryonic and larval fish are still nourished by the remnants of their yolk sac. All procedures conform to the National Institutes of Health guidelines regarding animal experimentation and were approved by Cornell University's Institutional Animal Care and Use Committee.

Immunostaining. Standard whole-mount antibody staining procedures were used as described previously (Higashijima et al., 2004b; McLean and Fetcho, 2004). After fixation with 4% paraformaldehyde, the whole brain was carefully excised to allow for better penetration of the antibodies. The engrailed1 staining was performed with a rabbit anti-En1 antibody (A gift from A. Joyner, Sloan-Kettering Institute, New York, NY; 1:250-1:500) and signal was detected with goat anti-rabbit antibody conjugated with HRP (Invitrogen, Carlsbad, CA; 1:200) and Alexa Fluor 647-Tyramide system (Invitrogen). The chx10 staining was performed with a guinea pig anti-chx10 antibody (1:2000) that was generated using bacterially-expressed proteins (Kimura et al., 2006), followed by a goat anti-guinea pig antibody conjugated with Alexa Fluor 633 (Invitrogen; 1:500). Both of the antibodies were shown to label neuronal populations in the zebrafish spinal cord identical to those detected by *in situ* hybridization for *eng1b* (Higashijima et al., 2004b) and alx (*chx10)* (Kimura et al., 2006), respectively.

Stochastic labeling

Stochastic labeling was performed as described previously (Higashijima et al., 2004a). Briefly, single cell embryos were positioned in wells within an agar plate (1.5% DNA-grade agarose in 10% Hanks with methylene blue). To label early born neurons, injections of small volumes of constructs (30ng/uL for each construct when

injecting two simultaneously) were performed into single cells within 45 minutes of fertilization, before the first cell division. To label later differentiating neurons, embryos were injected into the yolk at a multiple-cell stage at or before the 1000 cell stage. Embryos were screened at either 3 or 4 dpf by using a Leica fluorescent dissecting scope to find embryos with only 1-3 cells labeled in the hindbrain.

Injected constructs included promoters for the glycine transporter 2, the vesicular glutamate transporter, and alx, all described in prior studies (Bae et al., 2009; Higashijima et al., 2004a; Kimura et al., 2006; McLean et al., 2007). These were used to drive expression of fluorescent proteins as described in the text. For Brainbow labeling, three DNA constructs containing the following genes were mixed to a final concentration of 30 ng/ul each: UAS:Brainbow-1.1m (flanked by Tol-2 sites) (Livet et al., 2007), alx:Gal-4 (BAC), and CMV:CRE. Two uL of the DNA mixture was added to 1.5 ul Tol-2 mRNA and subsequently injected into alx:GFP nacre (Lister et al., 1999) embryos at the single cell stage. Fish positive for Brainbow-1.1m were imaged on the confocal, from hindbrain down to the spinal cord at 6 dpf to reconstruct the entire labeled neurons.

Transgenic lines

The transgenic lines we used included ones described in prior studies (Bae et al., 2009; Kimura et al., 2006; McLean et al., 2007), as well as two new ones with the promoters dbx1b and barhl2. These new lines, Tg(dbx1b:GFP) and Tg(barhl2:GFP) were constructed using the BACs zK17G17 and zC15L16, by a previously described method (Kimura et al., 2006) . The detailed approaches for generating these lines will be described elsewhere.

Confocal imaging

Confocal imaging was performed as described previously (Hale et al., 2001; McLean et al., 2008). Transgenic zebrafish were anaesthetized in 0.02% MS222 and embedded in 1.4% low melting point agar, typically with the dorsal side down and resting against a glass coverslip floor of a small petri dish. The agar was covered with 0.02% MS222 solution in 10% Hanks to prevent desiccation. Images were collected using an inverted Zeiss LSM confocal microscope with a Zeiss C-Apochromat 40X water lens. Green fluorescence was excited using 488 nm laser light and red fluorescence using a 543 nm laser. Green fluorescence emission was typically collected with band pass emission filters (505-530 nm or 505-550 nm) and red fluorescence emission was collected using a long pass 560 nm filter. Single image stacks were collected throughout the dorsoventral extent of hindbrain or spinal cord and generally collection last 40 minutes to 1.5 hours. To prevent photo damage, images were collected with high gain settings and averaged. Fish remained healthy and anaesthetized during this time.

Colocalization

Confocal image stacks containing green and red channels were observed using Imaris software (Bitplane). Using the colocalization add-on, minimum thresholds were determined for red and green channels slightly above noise levels for each channel.

We ensured that the dimmest cells were not thresholded out. A new channel was generated that represented co-labeled signal. For image stacks with low noise levels in both channels, the automated colocalization feature in Imaris was adequate for our purposes, but in noisier data sets thresholds were adjusted by hand to be sure that the thresholds were above the background noise.

Neuronal tracing and location measurements

Neurons were traced using the filament reconstruction feature provided in the Imaris software package (Bitplane). For image stacks with low background noise levels, automated reconstructions were performed choosing a diameter for a starting point (cell body) and a minimum diameter for end points along projections from the starting point. A threshold was used to adjust the number of start and end points for optimal tracing of single neurons. In cases where background noise levels were high, the autodepth feature of the Imaris filament software was used to trace neurons by hand along various two-dimensional planes transecting the three-dimensional volume, while allowing the program to determine the depth of the tracing. Reconstructions were constantly verified to be accurate representations of the labeled cell, and were used for illustration in this study because fine processes were hard to depict in two-dimensional projections of confocal image stacks. The dorsoventral position of a particular cell within a stripe was determined by dividing the distance of the middle of the cell body to the bottom of the stripe by the length of the entire stripe.

Photoconversion and analysis:

Huc:Kaede and alx:Kaede transgenic embryos (Kimura et al., 2006; Sato et al., 2006) were illuminated with UV light using a mercury bulb source for 10-40 seconds within their chorion. Immediately afterwards, photoconversion was confirmed by observation of the presence of red expression and an absence of green expression using green and red filters. Photoconverted fish were then kept at 28.5°C in a light-tight container until the day of imaging.

In order to determine which cells were exclusively green, and thus not expressing Kaede at the time of photoconversion, a colocalization was performed between the red and green channels (see colocalization section of Methods) and a new channel was constructed. A mask of this new channel was used to remove all of the green expression from colocalized regions to produce the images shown in Figure 4D.

For quantification of intensities in the neuropil, analysis was performed in Matlab. Horizontal confocal image stacks were rotated by 90 degrees using Imaris software to obtain cross sections. Neuropil regions were cropped in cross section and a series of tiffs within a local region including the dorsoventral and mediolateral extent of the labeled neuropil was generated in Imaris and was analyzed using Matlab (generally 15-100 slices). To generate a single image of this region, tiffs were summed and divided by the number of sections to show an averaged image plane of red and green intensities. To quantify the dorsoventral extent of red and green expression, voxels at the same dorsoventral position were summed across the mediolateral extent to obtain the intensity at a given dorsoventral location. Each value was divided by the maximum value of the distribution to generate a normalized distribution because the absolute intensity differences between red and green expression might be related to imaging conditions and not differences in the

distribution of red and green.

Targeted whole-cell patching of alx neurons in exposed brain preparation for input resistance measurements.

Larvae were anesthetized in 3-aminobenzoic acid ethyl ester (0.02% in Hank's solution) and then immobilized using alpha-bungarotoxin (Sigma-aldrich; 0.1% in Hank's solution). In order to measure input resistance of alx neurons in hindbrain, we initially used a dissection procedure similar to one described previously (Drapeau et al., 1999). We later switched to a less extensive exposure of the brain, leaving more of the head, including the eyes, intact to minimize potential damage to the neurons. Procedures for whole-cell recordings are described in the next section. After the electrophysiological measurements, the preparation was fixed with 4% formaldehyde with the pipette in place to avoid the movement of the cell body during the retraction of pipette. Then a z stack was acquired with a confocal microscope (LSM 510 META, Zeiss) for the measurement of the soma position relative to the alx stripe.

In vivo whole cell recordings in the hindbrain

Whole cell recordings were done in current clamp mode in 5dpf alx:GFP nacre transgenic larvae using modifications of methods described previously (Bhatt et al., 2007; Drapeau et al., 1999; Masino and Fetcho, 2005; McLean et al., 2007). Larvae were anesthetized using 3-aminobenzoic acid ethyl ester (MS-222, 0.02% in Hank's solution), paralyzed with alpha-bungarotoxin (1mg/ml in extracellular solution) and pinned twice through the notocord with tungsten pins to Sylgard in a small petri dish. The skin was removed from axial muscle between the pins for later ventral root recordings. The head was then rotated 90 degrees and pinned through the mouth. A small incision was made in the skin along a dorsal portion of the head for ease of patch electrode insertion. The dish, containing extracellular saline solution (134 mmol l–1,NaCl, 2.9 mmol l–1 KCl, 1.2 mmol l–1 MgCl2, 10mmol l–1 HEPES, 10 mmol l–1 glucose and 2.1 mmol l–1 CaCl2; adjusted to pH 7.8 with NaOH), was placed on a compound microscope (BX51WI; Olympus, Melville, NY) and a glass microelectrode, filled with extracellular solution was placed over an intermyotomal cleft where the axial skin was removed. A MultiClamp 700A amplifier (Axon Instruments) was used to monitor extracellular signals in current clamp mode at a gain of 1000, with the low- and high-frequency cutoff set at 300 and 5000 Hz, respectively.

Patch-clamp electrodes were pulled from thin-walled glass capillaries to 10-20 MΩ resistances. To record from hindbrain neurons, the electrodes were filled with intracellular saline solution (ionic composition in mmol l-1: 125 K-gluconate, 2.5 MgCl2, 10 EGTA, 10 HEPES, 4 Na2ATP; 6.25mg sulfur rhodamine-B, adjusted to pH 7.3 with KOH) and then gently advanced into the brain using motorized micromanipulators (Sutter Instrument Co.or Luigs- Neumann). Constant positive pressure (~20 mmHg) was applied to the micropipette using a pneumatic transducer (Bio-Tek Instruments Inc., Winooski, VT) until the tip of the electrode was brought within close proximity to a cell body. Cell bodies were visualized using differential interference contrast (DIC) optics, and the alx postive identity of a cell was confirmed

by briefly switching to an attenuated epifluorescent light source. A GΩ seal was then obtained either by equilibrating the micropipette to atmosphere or by applying gentle suction. A holding current of -65 mV was applied once the micropipette had become cell-attached and the membrane was penetrated with suction pulses. Whole cell current clamp recordings were made with a MultiClamp 700A amplifier (Axon Instruments) at a gain of 20 (Rf = 500mΩ) filtered at 30 kHz and digitized at 63 kHz.

Calcium imaging

Transgenic 4dpf alx:DsRed Casper fish (White et al., 2008) were first anesthetized using 3-aminobenzoic acid ethyl ester (MS-222, 0.02% in Hank's solution) and embedded in low melting point agarose (1.6% in Hank's solution, Sigma, St Louis, MO). A patch electrode (5-10MΩ resistance) was filled with 20% Oregon Green BAPTA-1 (10,000MW, Invitrogen/ Molecular Probes, Carlsbad, CA) and the indicator was electroporated along the dorsoventral axis of the alx stripe in caudal hindbrain by using a single cell Axoporator (-4V, 20ms duration square pulse, Axon Instruments). Larvae were then removed from the agarose, placed in a petri dish containing Hank's solution and stored in an incubator (28.5ºC) overnight.

The following day, we imaged the calcium indicator in hindbrain on a Zeiss LSM 510 inverted confocal microscope while recording from a ventral root using methods similar to those applied previously (McLean et al., 2007; McLean and Fetcho, 2009) . The larva was oriented on its side, with the head at 90 degrees relative to the tail, and pinned in place. Once a stable root recording was in place, the hindbrain was imaged. A time series capturing OGB-1 and alx:DsRed transgenic fluorescence was acquired while simultaneously monitoring ventral root activity. Swimming often occurred spontaneously, but was also elicited by either flashes of blue light or a brief electrical stimulus applied to the end of the tail. Following each experiment, we acquired high quality image stacks of the hindbrain for later reconstruction and cell positioning.

Analysis of calcium imaging and ventral root recordings was performed using custom written MatLab software. ROIs were selected to include single cells for measuring fluorescence intensity as an indicator of neuronal activity. The ventral root bursts were used to estimate swimming frequency during this activity, measured as the reciprocal of the period between the start of each successive burst. Due to the coarse temporal resolution of calcium imaging, we took a conservative approach to the measure of minimum swimming frequency at which a neuron was recruited, similar to McLean et al. 2007 (McLean et al., 2007). For each swimming episode in which a neuron showed a calcium response (defined as >9% fluorescence increase over baseline), the fastest swimming frequency during that episode was recorded. We then averaged the lowest three of these values to estimate the minimum speed of recruitment, being sure to bracket the lowest frequency of recruitment by having episodes in which the neurons did not respond.

Image stacks were then reconstructed in 3D using Imaris software (Bitplane). Neurons that were active during the experiment were identified and isosurfaces were generated for each. The length of the left and right stripes (at the position of the cell body) were each measured three times and averaged. The distance from the top of the

stripe to the center of the cell body was then measured three times and averaged. This distance along the dorsoventral axis of the stripe was then normalized for total stripe length at the position of the cell body.

References:

Al-Mosawie, A., Wilson, J.M., and Brownstone, R.M. (2007). Heterogeneity of V2-derived interneurons in the adult mouse spinal cord. Eur J Neurosci *26*, 3003-3015.

Altman, J., and Bayer, S.A. (1980). Development of the brain stem in the rat. IV. Thymidine-radiographic study of the time of origin of neurons in the pontine region. J Comp Neurol *194*, 905-929.

Alvarez, F.J., Jonas, P.C., Sapir, T., Hartley, R., Berrocal, M.C., Geiman, E.J., Todd, A.J., and Goulding, M. (2005). Postnatal phenotype and localization of spinal cord V1 derived interneurons. J Comp Neurol *493*, 177-192.

Ando, R., Hama, H., Yamamoto-Hino, M., Mizuno, H., and Miyawaki, A. (2002). An optical marker based on the UV-induced green-to-red photoconversion of a fluorescent protein. Proc Natl Acad Sci U S A *99*, 12651-12656.

Bae, Y.K., Kani, S., Shimizu, T., Tanabe, K., Nojima, H., Kimura, Y., Higashijima, S., and Hibi, M. (2009). Anatomy of zebrafish cerebellum and screen for mutations affecting its development. Dev Biol *330*, 406-426.

Bhatt, D.H., McLean, D.L., Hale, M.E., and Fetcho, J.R. (2007). Grading movement strength by changes in firing intensity versus recruitment of spinal interneurons. Neuron *53*, 91-102.

Briscoe, J., Pierani, A., Jessell, T.M., and Ericson, J. (2000). A homeodomain protein code specifies progenitor cell identity and neuronal fate in the ventral neural tube. Cell *101*, 435-445.

Cepeda-Nieto, A.C., Pfaff, S.L., and Varela-Echavarria, A. (2005). Homeodomain transcription factors in the development of subsets of hindbrain reticulospinal neurons. Mol Cell Neurosci *28*, 30-41.

Clarke, J.D., and Lumsden, A. (1993). Segmental repetition of neuronal phenotype sets in the chick embryo hindbrain. Development *118*, 151-162.

Colombo, A., Reig, G., Mione, M., and Concha, M.L. (2006). Zebrafish BarH-like genes define discrete neural domains in the early embryo. Gene Expr Patterns *6*, 347-352.

Crone, S.A., Quinlan, K.A., Zagoraiou, L., Droho, S., Restrepo, C.E., Lundfald, L., Endo, T., Setlak, J., Jessell, T.M., Kiehn, O., and Sharma, K. (2008). Genetic ablation of V2a ipsilateral interneurons disrupts left-right locomotor coordination in mammalian spinal cord. Neuron *60*, 70-83.

de Vries, J., Visser, G., and Prechtl, H. (1982). The emergence of fetal behaviour.

I. Qualitative aspects. Early Hum Dev *7*, 301-322.

Drapeau, P., Ali, D.W., Buss, R.R., and Saint-Amant, L. (1999). In vivo recording from identifiable neurons of the locomotor network in the developing zebrafish. J Neurosci Methods *88*, 1-13.

Faber, D.S., Fetcho, J.R., and Korn, H. (1989). Neuronal networks underlying the escape response in goldfish. General implications for motor control. Ann N Y Acad Sci *563*, 11-33.

Fetcho, J.R. (1992). Excitation of motoneurons by the Mauthner axon in goldfish: complexities in a "simple" reticulospinal pathway. J Neurophysiol *67*, 1574-1586.

Fetcho, J.R., and Faber, D.S. (1988). Identification of motoneurons and interneurons in the spinal network for escapes initiated by the mauthner cell in goldfish. J Neurosci *8*, 4192-4213.

Fetcho, J.R., and Svoboda, K.R. (1993). Fictive swimming elicited by electrical stimulation of the midbrain in goldfish. J Neurophysiol *70*, 765-780.

Fjose, A., Izpisua-Belmonte, J.C., Fromental-Ramain, C., and Duboule, D. (1994). Expression of the zebrafish gene hlx-1 in the prechordal plate and during CNS development. Development *120*, 71-81.

Garcia-Campmany, L., Stam, F.J., and Goulding, M. (2010). From circuits to behaviour: motor networks in vertebrates. Curr Opin Neurobiol *20*, 116-125.

Gosgnach, S., Lanuza, G.M., Butt, S.J., Saueressig, H., Zhang, Y., Velasquez, T., Riethmacher, D., Callaway, E.M., Kiehn, O., and Goulding, M. (2006). V1 spinal neurons regulate the speed of vertebrate locomotor outputs. Nature *440*, 215-219.

Hale, M.E., Ritter, D.A., and Fetcho, J.R. (2001). A confocal study of spinal interneurons in living larval zebrafish. J Comp Neurol *437*, 1-16.

Hanneman, E., Trevarrow, B., Metcalfe, W.K., Kimmel, C.B., and Westerfield, M. (1988). Segmental pattern of development of the hindbrain and spinal cord of the zebrafish embryo. Development *103*, 49-58.

Higashijima, S., Mandel, G., and Fetcho, J.R. (2004a). Distribution of prospective glutamatergic, glycinergic, and GABAergic neurons in embryonic and larval zebrafish. J Comp Neurol *480*, 1-18.

Higashijima, S., Masino, M.A., Mandel, G., and Fetcho, J.R. (2004b). Engrailed-1 expression marks a primitive class of inhibitory spinal interneuron. J Neurosci *24*, 5827-5839.

Higashijima, S., Schaefer, M., and Fetcho, J.R. (2004c). Neurotransmitter properties of spinal interneurons in embryonic and larval zebrafish. J Comp Neurol *480*, 19-37.

Kimura, Y., Okamura, Y., and Higashijima, S. (2006). alx, a zebrafish homolog of Chx10, marks ipsilateral descending excitatory interneurons that participate in the regulation of spinal locomotor circuits. J Neurosci *26*, 5684-5697.

Lanuza, G.M., Gosgnach, S., Pierani, A., Jessell, T.M., and Goulding, M. (2004). Genetic identification of spinal interneurons that coordinate left-right locomotor activity necessary for walking movements. Neuron *42*, 375-386.

Li, W.C., Higashijima, S., Parry, D.M., Roberts, A., and Soffe, S.R. (2004). Primitive roles for inhibitory interneurons in developing frog spinal cord. J Neurosci *24*, 5840-5848.

Li, W.C., Soffe, S.R., Wolf, E., and Roberts, A. (2006). Persistent responses to brief stimuli: feedback excitation among brainstem neurons. J Neurosci *26*, 4026-4035.

Liao, J.C., and Fetcho, J.R. (2008). Shared versus specialized glycinergic spinal interneurons in axial motor circuits of larval zebrafish. J Neurosci *28*, 12982-12992.

Lingenhohl, K., and Friauf, E. (1994). Giant neurons in the rat reticular formation: A sensorimotor interface in the elementary acoustic startle circuit. J.Neurosci. *14*, 1176-1194.

Lister, J.A., Robertson, C.P., Lepage, T., Johnson, S.L., and Raible, D.W. (1999). nacre encodes a zebrafish microphthalmia-related protein that regulates neural-crest-derived pigment cell fate. Development *126*, 3757-3767.

Liu, D.W., and Westerfield, M. (1988). Function of identified motoneurones and co-ordination of primary and secondary motor systems during zebra fish swimming. J Physiol *403*, 73-89.

Liu, K.S., and Fetcho, J.R. (1999). Laser ablations reveal functional relationships of segmental hindbrain neurons in zebrafish. Neuron *23*, 325-335.

Livet, J., Weissman, T.A., Kang, H., Draft, R.W., Lu, J., Bennis, R.A., Sanes, J.R., and Lichtman, J.W. (2007). Transgenic strategies for combinatorial expression of fluorescent proteins in the nervous system. Nature *450*, 56-62.

Masino, M.A., and Fetcho, J.R. (2005). Fictive swimming motor patterns in wild type and mutant larval zebrafish. J Neurophysiol *93*, 3177-3188.

McLean, D.L., Fan, J., Higashijima, S., Hale, M.E., and Fetcho, J.R. (2007). A topographic map of recruitment in spinal cord. Nature *446*, 71-75.

McLean, D.L., and Fetcho, J.R. (2004). Ontogeny and innervation patterns of dopaminergic, noradrenergic, and serotonergic neurons in larval zebrafish. J Comp Neurol *480*, 38-56.

McLean, D.L., and Fetcho, J.R. (2009). Spinal interneurons differentiate sequentially from those driving the fastest swimming movements in larval zebrafish to those driving the slowest ones. J Neurosci *29*, 13566-13577.

McLean, D.L., Masino, M.A., Koh, I.Y., Lindquist, W.B., and Fetcho, J.R. (2008). Continuous shifts in the active set of spinal interneurons during changes in locomotor speed. Nat Neurosci *11*, 1419-1429.

Moreno, N., Bachy, I., Retaux, S., and Gonzalez, A. (2005). LIM-homeodomain genes as territory markers in the brainstem of adult and developing Xenopus laevis. J Comp Neurol *485*, 240-254.

O'Malley, D.M., Kao, Y.H., and Fetcho, J.R. (1996). Imaging the functional organization of zebrafish hindbrain segments during escape behaviors. Neuron *17*, 1145-1155.

Passini, M.A., Raymond, P.A., and Schechter, N. (1998). Vsx-2, a gene encoding a paired-type homeodomain, is expressed in the retina, hindbrain, and spinal cord during goldfish embryogenesis. Brain Res Dev Brain Res *109*, 129-135.

Pierani, A., Moran-Rivard, L., Sunshine, M.J., Littman, D.R., Goulding, M., and Jessell, T.M. (2001). Control of interneuron fate in the developing spinal cord by the progenitor homeodomain protein Dbx1. Neuron *29*, 367-384.

Rachidi, M., and Lopes, C. (2006). Differential transcription of Barhl1 homeobox gene in restricted functional domains of the central nervous system suggests a role in brain patterning. Int J Dev Neurosci *24*, 35-44.

Sato, T., Takahoko, M., and Okamoto, H. (2006). HuC:Kaede, a useful tool to label neural morphologies in networks in vivo. Genesis *44*, 136-142.

Saueressig, H., Burrill, J., and Goulding, M. (1999). Engrailed-1 and netrin-1 regulate axon pathfinding by association interneurons that project to motor neurons. Development *126*, 4201-4212.

Schubert, F.R., Dietrich, S., Mootoosamy, R.C., Chapman, S.C., and Lumsden, A. (2001). Lbx1 marks a subset of interneurons in chick hindbrain and spinal cord. Mech Dev *101*, 181-185.

Storm, R., Cholewa-Waclaw, J., Reuter, K., Brohl, D., Sieber, M., Treier, M., Muller, T., and Birchmeier, C. (2009). The bHLH transcription factor Olig3 marks the dorsal neuroepithelium of the hindbrain and is essential for the development of brainstem nuclei. Development *136*, 295-305.

Thaeron, C., Avaron, F., Casane, D., Borday, V., Thisse, B., Thisse, C., Boulekbache, H., and Laurenti, P. (2000). Zebrafish evx1 is dynamically expressed during embryogenesis in subsets of interneurones, posterior gut and urogenital system. Mech Dev *99*, 167-172.

Tumpel, S., Wiedemann, L.M., and Krumlauf, R. (2009). Hox genes and segmentation of the vertebrate hindbrain. Curr Top Dev Biol *88*, 103-137.

White, R.M., Sessa, A., Burke, C., Bowman, T., LeBlanc, J., Ceol, C., Bourque, C., Dovey, M., Goessling, W., Burns, C.E., and Zon, L.I. (2008). Transparent adult zebrafish as a tool for in vivo transplantation analysis. Cell Stem Cell *2*, 183-189.

Wilkinson, D.G., Bhatt, S., Cook, M., Boncinelli, E., and Krumlauf, R. (1989). Segmental expression of Hox-2 homoeobox-containing genes in the developing mouse hindbrain. Nature *341*, 405-409.

Wullimann, M.F., Rupp, B., and Reichert, H. (1996). Neuroanatomy of the Zebrafish Brain: A Topological Atlas (Basel: Birkhauser).

Zhang, Y., Narayan, S., Geiman, E., Lanuza, G.M., Velasquez, T., Shanks, B., Akay, T., Dyck, J., Pearson, K., Gosgnach, S., *et al*. (2008). V3 spinal neurons establish a robust and balanced locomotor rhythm during walking. Neuron *60*, 84-96.

Figure legends:

Figure 1. Interleaved stripes of neurons in hindbrain marked by transmitter phenotype. A: Location of images shown in this figure. All images are reconstructed cross sections from confocal image stacks acquired *in vivo* from a 4 dpf fish. B: Cross sections (approximately 30 micron thickness) of dual expression vglut:DsRed x glyt2:GFP transgenic fish at 4 dpf. Glycinergic and glutamatergic neurons form interleaved stripes that alternate from medial to lateral and are present throughout hindbrain. In B1, red/green arrows indicate ventral regions of each stripe of glutamatergic (red) and glycinergic (green) neurotransmitter type. B1-B4: stripes within rhombomere 8, rhombomere 7, rhombomere 6, and rhombomere 4, respectively. Dorsal is at the top for all images. Scale bars = 20 um. (C) Summary of neurotransmitter stripe patterning in hindbrain.

Figure 2 Relationships between transcription factor expression patterns and transmitter stripes. A-D: Transcription factor stripes are present in hindbrain and overlap glutamatergic and glycinergic stripes. All images are reconstructed cross sections from confocal images acquired *in vivo*. A1-2: Images of green (A1) and red (A2) channels from a vglut:DsRed x alx:GFP transgenic fish imaged *in vivo* at 3 dpf in rhombomere 7/8. A3: Colocalization of alx:GFP and vglut:DsRed (A3) indicates that all medial glutamate stripe neurons express the alx transcription factor. B: Images of engrailed-1 immunostaining (B1) in the glyt2 transgenic line (B2, shown in red here) from rhombomere 7 in a 5 dpf fish. B3: Colocalization of engrailed-1 immunoreactivity and glyt2:GFP expression reveals that all medial glycine stripe neurons express engrailed-1. C: Images of green (C1) and red channels (C2) from rhombomere 7 in a 4 dpf vglut:DsRed x dbx1b:GFP transgenic fish indicate that neurons in the middle glutamate stripe are dbx1b positive, as confirmed by the colocalization in C3. The glutamatergic dbx1b neurons are medially positioned within

the dbx1b labeling, with other dbx1b positive, non-glutamatergic neurons located more laterally in a region known to contain glycinergic neurons. D1-2: Images of green (D1) and red channels (D2) from rhombomere 8 from a 4 dpf transgenic fish (vglut:DsRed x barhl2:GFP) indicate that barhl2 staining overlaps a portion of the most lateral glutamatergic populations. Colocalization of barhl2:GFP and vglut:DsRed (D3) shows that the lateral neurons within the lateral glutamate stripe express the barhl2 transcription factor. Right most panels in A-D: Red/green bars illustrate positions of glutamate (red) and glycine (green) stripes. Black bars indicate the location of the transcription factor expression relative to the neurotransmitter stripes. E1-E5: Optical sections from an alx:DsRed x barhl2:GFP transgenic fish to show the change in the relationships between transcription patterning from spinal cord into hindbrain. The locations of the sections are shown on the right. Scale bars = 20 um in all images.

Figure 3 Morphology of neurons in the neurotransmitter stripes. All panels show horizontal projections of single-neuron reconstructions from different fish sorted by stripe location. A: Neurons in the medial glutamatergic stripe. The descending axons of the neurons often extend into spinal cord and are truncated here (see also Fig. 5A). B: Neurons in the most medial glycinergic stripe. C: Neurons in the middle glycinergic stripe. D: Neurons in the lateral glycinergic stripe. All panels show single cell 3D reconstructions of neurons in 5-6dpf fish label by stochastic expression of membrane targeted GFP or RFP in transgenic lines with transmitter or transcription factor stripes labeled in a different color. Reconstructions are shown in a dorsal view, with rostral to the top. Neurons have been oriented with the cell body to the left of the midline. For A and B, lateral is to the left and medial is to the right. In A and B, dotted lines mark the continuation of truncated axons. In C and D, dotted lines indicate the approximate position of the midline of the fish, or, in one instance, the continuation of an axon. In each panel, the left column illustrates the stripe containing the cells (all identified with colocalized expression of stochastic labeling and neurotransmitter/transcription factor promoter driven fluorescence). Scale bars=20μm.

Figure 4. Age-related patterning within the medial glutamatergic, alx hindbrain stripe. A: Orientation of images. B: Timing of experiments. In C, a lateral view of a photoconverted fish is shown from hindbrain through to spinal cord; this is a montage of three image stacks. White dashed lines indicate the rostrocaudal locations of the numbered cross sections. In most cases, the oldest neurons are ventrally positioned, with younger ones more dorsally positioned within the stripe. Two exceptions are indicated by asterisks within rhombomeres 6 and 8 in which either the age-ordering (R6) or stripe patterning (R8) is different . D: Lateral views of hindbrain/spinal cord regions of alx:Kaede transgenic fish photoconverted/imaged at different times (timing shown in B). In each case, green expression is removed from red cells; therefore, green indicates cells that are uniquely green; yellow arises from overlap of green and red somata in the projection. In all three cases, the vast majority of these younger

neurons are more dorsally positioned within the alx stripe. The green below the red neurons (yellow region) in D1 is largely processes in the neuropil from the massive number of green somata in the stripe. E1: Reconstructed confocal cross section shows that neuropil for older neurons (red) tends to be dorsal to that for younger neurons (green). E2: Quantification of red/green expression within neuropil. A neuropil volume was extracted from a confocal image and a raw sum of red/green neuropil expression in different lines from ventral to dorsal was calculated and normalized by the maximum intensity to obtain the relative intensity in each color at different postions. Red expression is shifted dorsally relative to more ventral green expression in E2 (rhombomere 7). F: Photoconversion of an alx:Kaede transgenic fish imaged in spinal cord also shows age-related separation in the neuropil. F1: a reconstructed confocal cross section shows that neuropil for older neurons (red) tends to be medial and dorsal to that younger neurons (green). F2: Quantification of the distribution of staining in the neuropil, as in E2. Scale bars = 20 um for all images except E2 and F2 where scale bars = 10 um.

Figure 5: Variation in morphology and input resistance along the axis of the medial glutamatergic, alx stripe. A: Example image of a reconstruction of an alx neuron from a montage of image stacks shown in lateral view with the head towards the left. The alx neurons are green and the labeled cell is highlighted red in a surface rendering of the traced neuron. B: 3D reconstructions of neurons from different dorsoventral locations in the medial glutamatergic stripe in rhombomere 7. Neurons are arranged with the most dorsal one at the top and their relative positions from the bottom of the stripe are: 0.51, 0.28 and 0.16. All neurons are shown in lateral view with rostral to the left and dorsal up. Their colors match colored points on the plots in 5D. C: Cross section image of a patched neuron in an alx:GFP transgenic fish to show how the location along the total stripe axis (white line) was measured. D: A plot of the total 3D axonal length of labeled neurons versus their dorsal ventral location in the stripe. More ventral neurons have systematically more axonal length ($p<0.0001$). Data from ten neurons are shown, but two of the points overlapped (open circle). Red, green, and blue points match the red, green, and blue reconstructions of the 3 neurons in 5B. E: Plot of the input resistance of a neuron versus its dorsoventral location in a stripe. More dorsal neurons have systematically higher input resistances in both more (black dots, $p<0.05$) and less exposed brain preparations (gray squares, $p<.0.01$). See text for further details. Scale bars = 200μm.

Figure 6. Activation patterns of neurons within the medial glutamatergic stripe during swimming. A: Patch recording of an alx:GFP expressing neuron in hindbrain segment 7 of a 5 dpf fish while simultaneously recording motor activity in a ventral root. Left side shows a cross section view in the region of the patched cell with alx neurons in green and the patched alx cell in red. Right: The patch recording from the alx cell on the left is shown below the simultaneous ventral root recording. The alx neuron shows rhythmic oscillations and fires during the swimming activity recorded in the ventral root. B: Examples of calcium imaging of the activation of alx neurons from different locations in the stripe at different frequencies of swimming in 5 dpf fish. Left side

shows the locations of the neurons relative to the stripes. Colored dots correspond to those on the plot in C. Right side shows calcium responses of the neurons on the left in two example trials at swimming frequencies near those when the neurons are first recruited. For example, the top neuron does not respond in a trial with peak frequency of 22Hz, but does at 24. C. Plot of the minimum swimming frequency at which a neuron responds (measured as described in methods) versus the dorsoventral location of the neuron. This plot includes both alx positive neurons and other non-alx positive neurons in the region of the alx stripe. Neurons in B are shown in color. D: Similar to the plot in C, but with the alx neurons in black and the non-alx cells in the same area in gray. Both show a similar relationship between recruitment and position, with neurons recruited from the top of the stripe down as the frequency of swimming rises.

Figure 7. Summary of the rules governing hindbrain patterning. A: Interleaved neurotransmitter stripes overlap with transcription factor expression patterns. Different neuronal morphologies shown on the right are associated (by matching colors here) with the different stripes. B: Within an individual stripe (alx stripe shown on the left), the somata of neurons are ordered along the axis of the stripe by age, the location of their processes in the neuropil, and their total axonal length. This order corresponds to systematic variation in their input resistance and order of recruitment during different speeds of swimming, which also map onto the axis of the stripe.

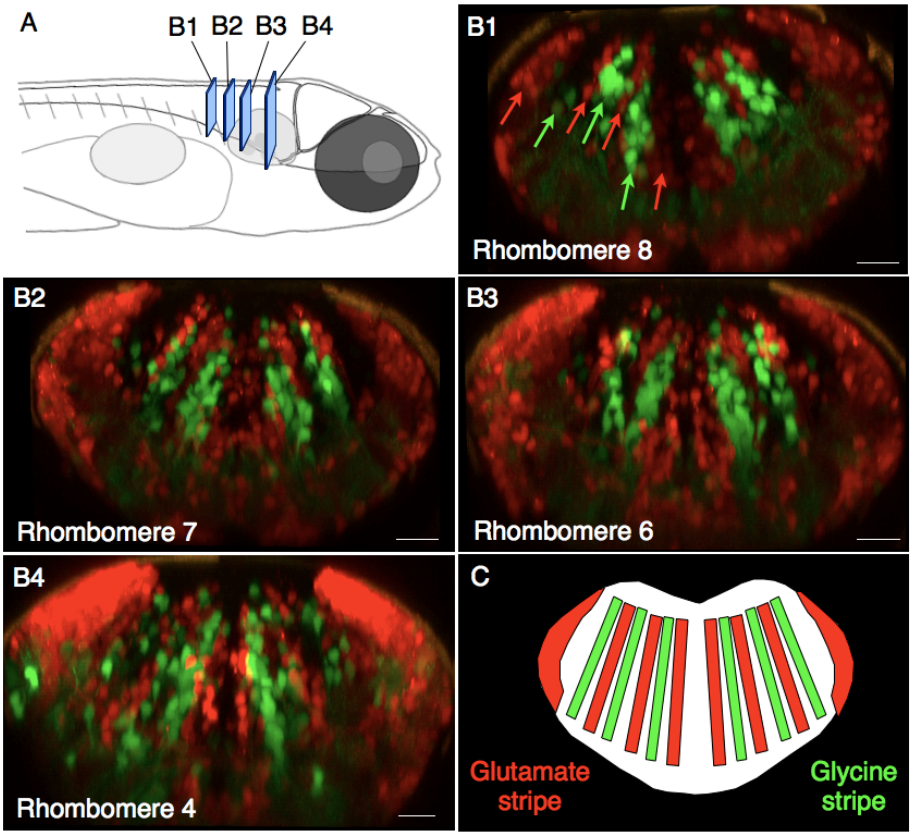

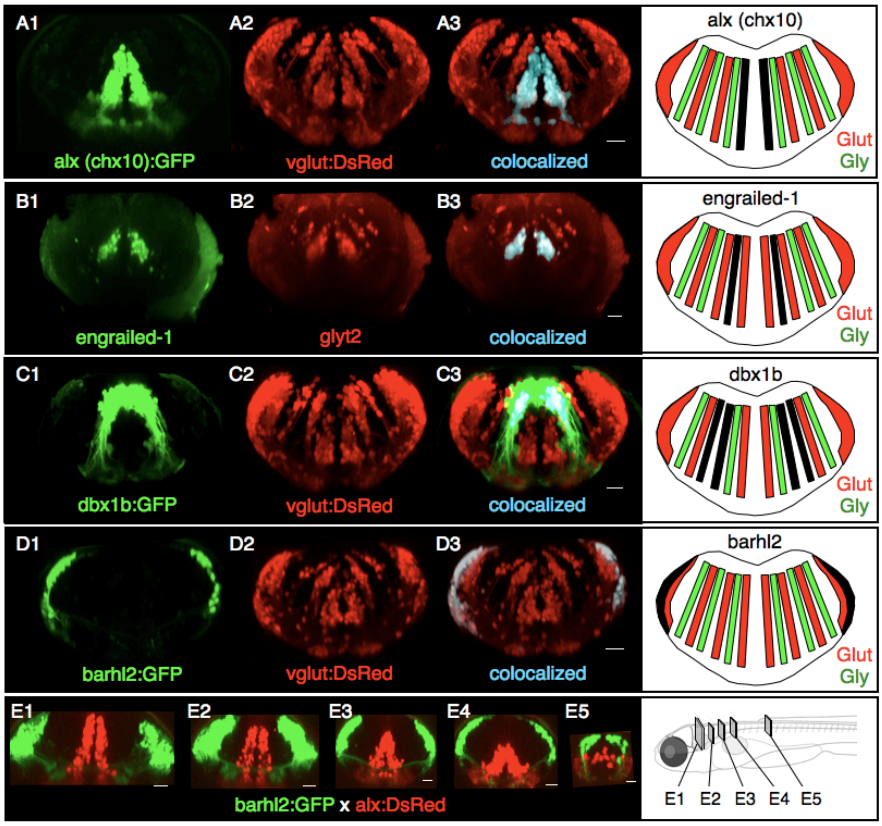
A1
A2
A3
alx (chx10):GFP
vglut:DsRed
colocalized
alx (chx10)
Glut
Gly
B1
B2
B3
engrailed-1
glyt2
colocalized
engrailed-1
Glut
Gly
C1
C2
C3
dbx1b:GFP
vglut:DsRed
colocalized
dbx1b
Glut
Gly
D1
D2
D3
barhl2:GFP
vglut:DsRed
colocalized
barhl2
Glut
Gly
E1
E2
E3
E4
E5
barhl2:GFP x alx:DsRed
E1 E2 E3 E4 E5

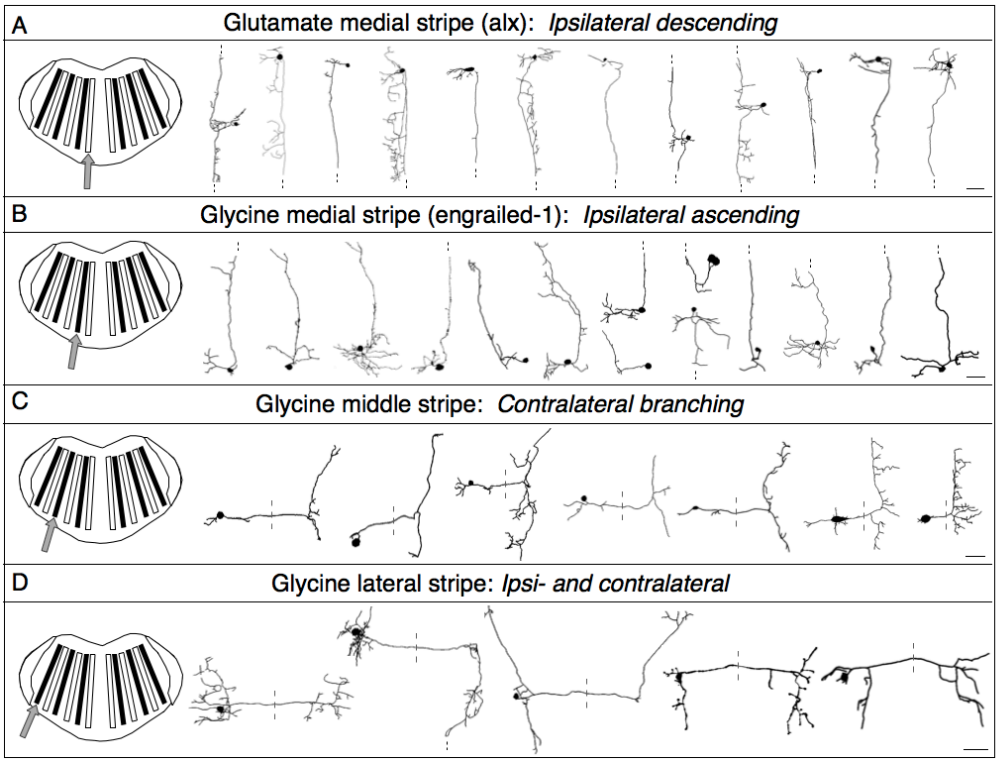
A
Glutamate medial stripe (alx): *Ipsilateral descending*
B
Glycine medial stripe (engrailed-1): *Ipsilateral ascending*
C
Glycine middle stripe: *Contralateral branching*
D
Glycine lateral stripe: *Ipsi- and contralateral*

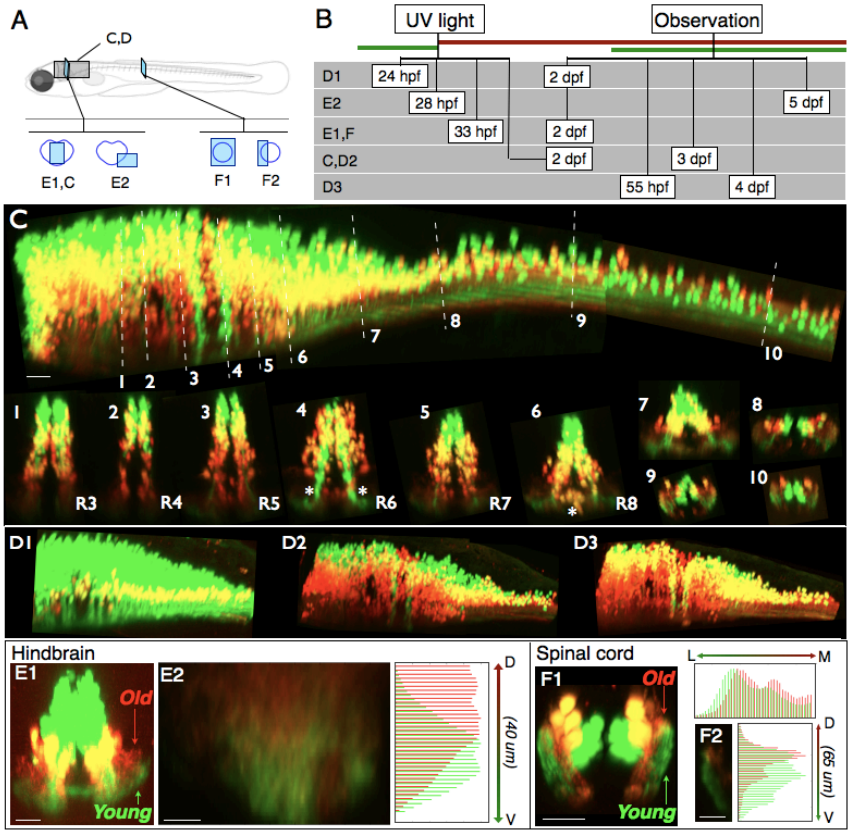
A
C,D
E1,C
E2
F1
F2
B
UV light
Observation
D1
24 hpf
2 dpf
E2
28 hpf
5 dpf
E1,F
33 hpf
2 dpf
C,D2
2 dpf
3 dpf
D3
55 hpf
4 dpf
C
1
2
3
4
5
6
7
8
9
10
R3
R4
R5
R6
R7
R8
D1
D2
D3
Hindbrain
E1
Old
Young
E2
D
(40 um)
V
Spinal cord
F1
Old
Young
L
M
F2
D
(65 um)
V

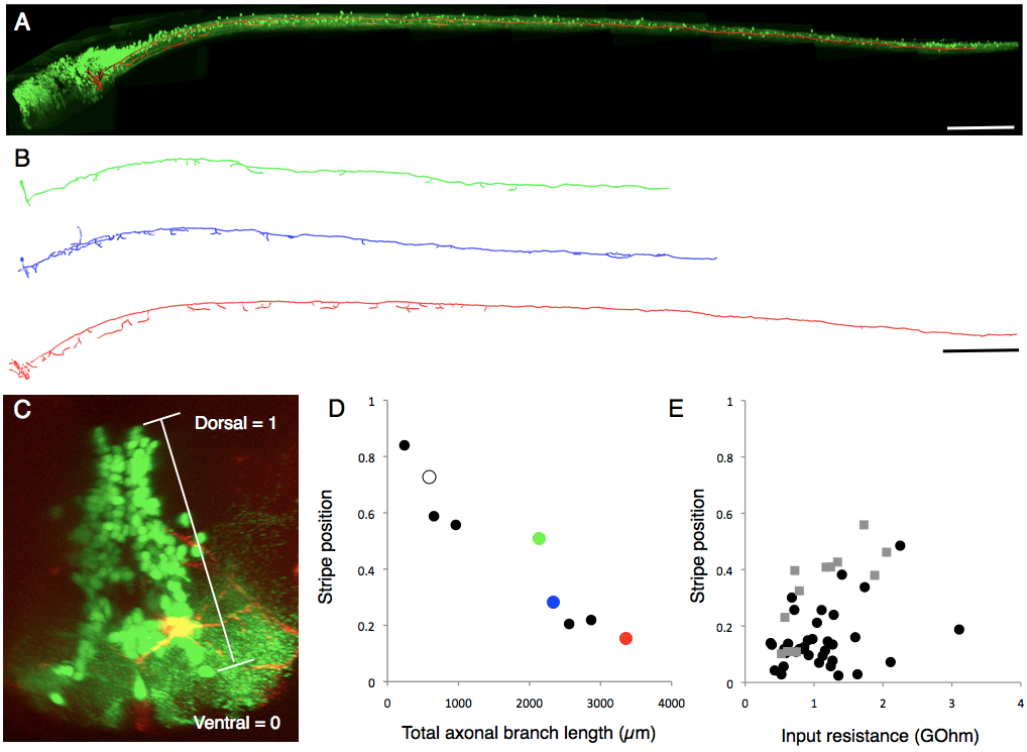
A
B
C
Dorsal = 1
Ventral = 0
D
Stripe position
Total axonal branch length (μm)
E
Stripe position
Input resistance (GOhm)

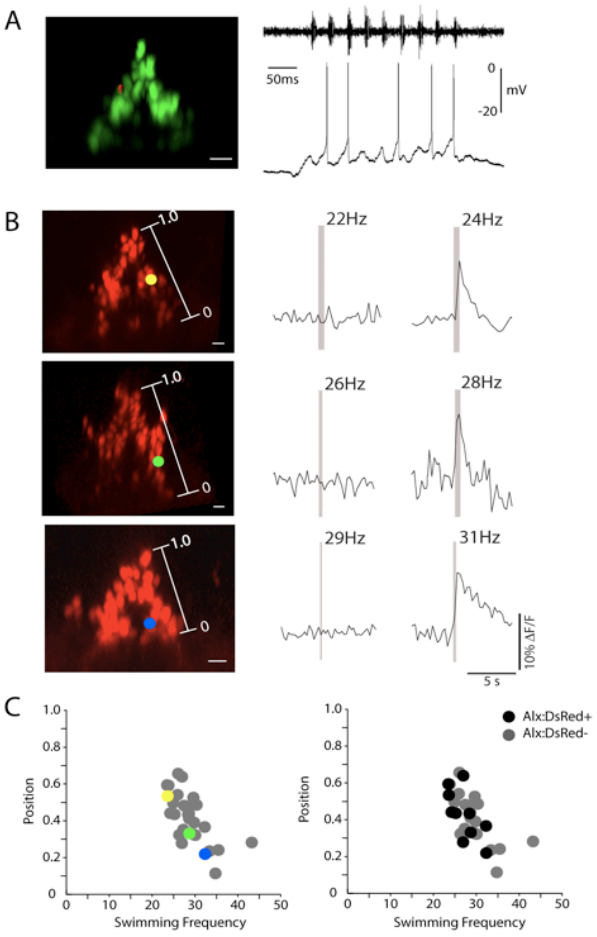
A
50ms
0
mV
-20
B
1.0
0
22Hz
24Hz
26Hz
28Hz
29Hz
31Hz
10% ΔF/F
5 s
C
Position
Swimming Frequency
Alx:DsRed+
Alx:DsRed-

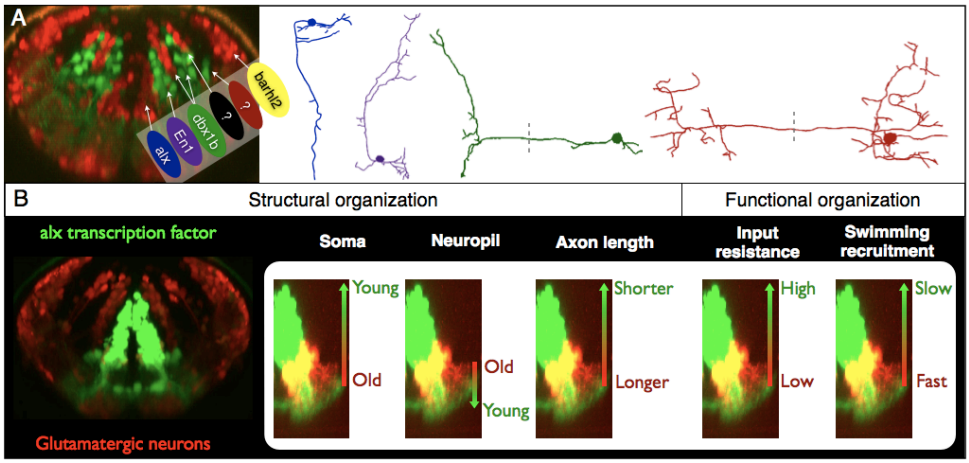
A
barhl2
?
dbx1b
En1
alx
B
Structural organization
Functional organization
alx transcription factor
Glutamatergic neurons
Soma
Neuropil
Axon length
Input resistance
Swimming recruitment
Young
Old
Old
Young
Shorter
Longer
High
Low
Slow
Fast

REFERENCES

1. Briscoe, J. and J. Ericson, The specification of neuronal identity by graded Sonic Hedgehog signalling. Semin Cell Dev Biol, 1999. 10(3): p. 353-62.
2. Briscoe, J., et al., A homeodomain protein code specifies progenitor cell identity and neuronal fate in the ventral neural tube. Cell, 2000. 101(4): p. 435-45.
3. Cepeda-Nieto, A.C., S.L. Pfaff, and A. Varela-Echavarria, Homeodomain transcription factors in the development of subsets of hindbrain reticulospinal neurons. Mol Cell Neurosci, 2005. 28(1): p. 30-41.
4. Clarke, J.D. and A. Lumsden, Segmental repetition of neuronal phenotype sets in the chick embryo hindbrain. Development, 1993. 118(1): p. 151-62.
5. Higashijima, S., G. Mandel, and J.R. Fetcho, Distribution of prospective glutamatergic, glycinergic, and GABAergic neurons in embryonic and larval zebrafish. J Comp Neurol, 2004. 480(1): p. 1-18.
6. Kinkhabwala, A.K., A novel patterning of interneurons in hindbrain reveals new principles of organization. 2009, Cornell University.
7. McLean, D.L., et al., A topographic map of recruitment in spinal cord. Nature, 2007. 446(7131): p. 71-5.
8. McLean, D.L. and J.R. Fetcho, Spinal interneurons differentiate sequentially from those driving the fastest swimming movements in larval zebrafish to those driving the slowest ones. J Neurosci, 2009. 29(43): p. 13566-77.
9. McLean, D.L., et al., Continuous shifts in the active set of spinal interneurons during changes in locomotor speed. Nat Neurosci, 2008. 11(12): p. 1419-29.
10. Pierani, A., et al., Control of interneuron fate in the developing spinal cord by the progenitor homeodomain protein Dbx1. Neuron, 2001. 29(2): p. 367-84.

11. Liem, K.F., Jr., G. Tremml, and T.M. Jessell, A role for the roof plate and its resident TGFbeta-related proteins in neuronal patterning in the dorsal spinal cord. Cell, 1997. 91(1): p. 127-38.
12. Goulding, M. and E. Lamar, Neuronal patterning: Making stripes in the spinal cord. Curr Biol, 2000. 10(15): p. R565-8.
13. Pierani, A., et al., A sonic hedgehog-independent, retinoid-activated pathway of neurogenesis in the ventral spinal cord. Cell, 1999. 97(7): p. 903-15.
14. Lanuza, G.M., et al., Genetic identification of spinal interneurons that coordinate left-right locomotor activity necessary for walking movements. Neuron, 2004. 42(3): p. 375-86.
15. Higashijima, S., et al., Engrailed-1 expression marks a primitive class of inhibitory spinal interneuron. J Neurosci, 2004. 24(25): p. 5827-39.
16. Li, W.C., et al., Primitive roles for inhibitory interneurons in developing frog spinal cord. J Neurosci, 2004. 24(25): p. 5840-8.
17. Sapir, T., et al., Pax6 and engrailed 1 regulate two distinct aspects of renshaw cell development. J Neurosci, 2004. 24(5): p. 1255-64.
18. Saueressig, H., J. Burrill, and M. Goulding, Engrailed-1 and netrin-1 regulate axon pathfinding by association interneurons that project to motor neurons. Development, 1999. 126(19): p. 4201-12.
19. Gosgnach, S., et al., V1 spinal neurons regulate the speed of vertebrate locomotor outputs. Nature, 2006. 440(7081): p. 215-9.
20. Alvarez, F.J., et al., Postnatal phenotype and localization of spinal cord V1 derived interneurons. J Comp Neurol, 2005. 493(2): p. 177-92.
21. Wenner, P., M.J. O'Donovan, and M.P. Matise, Topographical and physiological characterization of interneurons that express engrailed-1 in the embryonic chick spinal cord. J Neurophysiol, 2000. 84(5): p. 2651-7.

22. Jankowska, E., T.C. Fu, and A. Lundberg, Reciprocal La inhibition during the late reflexes evoked from the flexor reflex afferents after DOPA. Brain Res, 1975. 85(1): p. 99-102.
23. Kjaerulff, O. and O. Kiehn, Distribution of networks generating and coordinating locomotor activity in the neonatal rat spinal cord in vitro: a lesion study. J Neurosci, 1996. 16(18): p. 5777-94.
24. Karunaratne, A., et al., GATA proteins identify a novel ventral interneuron subclass in the developing chick spinal cord. Dev Biol, 2002. 249(1): p. 30-43.
25. Crone, S.A., et al., Genetic ablation of V2a ipsilateral interneurons disrupts left-right locomotor coordination in mammalian spinal cord. Neuron, 2008. 60(1): p. 70-83.
26. Thaler, J., et al., Active suppression of interneuron programs within developing motor neurons revealed by analysis of homeodomain factor HB9. Neuron, 1999. 23(4): p. 675-87.
27. Al-Mosawie, A., J.M. Wilson, and R.M. Brownstone, Heterogeneity of V2-derived interneurons in the adult mouse spinal cord. Eur J Neurosci, 2007. 26(11): p. 3003-15.
28. Lundfald, L., et al., Phenotype of V2-derived interneurons and their relationship to the axon guidance molecule EphA4 in the developing mouse spinal cord. Eur J Neurosci, 2007. 26(11): p. 2989-3002.
29. Barabino, S.M., et al., Inactivation of the zebrafish homologue of Chx10 by antisense oligonucleotides causes eye malformations similar to the ocular retardation phenotype. Mech Dev, 1997. 63(2): p. 133-43.
30. Kimura, Y., Y. Okamura, and S. Higashijima, alx, a zebrafish homolog of Chx10, marks ipsilateral descending excitatory interneurons that participate in

the regulation of spinal locomotor circuits. J Neurosci, 2006. 26(21): p. 5684-97.

31. Wilson, J.M., et al., Conditional rhythmicity of ventral spinal interneurons defined by expression of the Hb9 homeodomain protein. J Neurosci, 2005. 25(24): p. 5710-9.

32. Wilson, J.M., A.I. Cowan, and R.M. Brownstone, Heterogeneous electrotonic coupling and synchronization of rhythmic bursting activity in mouse Hb9 interneurons. J Neurophysiol, 2007. 98(4): p. 2370-81.

33. Ziskind-Conhaim, L., L. Wu, and E.P. Wiesner, Persistent sodium current contributes to induced voltage oscillations in locomotor-related hb9 interneurons in the mouse spinal cord. J Neurophysiol, 2008. 100(4): p. 2254-64.

34. Tazerart, S., L. Vinay, and F. Brocard, The persistent sodium current generates pacemaker activities in the central pattern generator for locomotion and regulates the locomotor rhythm. J Neurosci, 2008. 28(34): p. 8577-89.

35. Zhang, Y., et al., V3 spinal neurons establish a robust and balanced locomotor rhythm during walking. Neuron, 2008. 60(1): p. 84-96.

36. Baines, R.A., et al., Postsynaptic expression of tetanus toxin light chain blocks synaptogenesis in Drosophila. Curr Biol, 1999. 9(21): p. 1267-70.

37. Baines, R.A., et al., Altered electrical properties in Drosophila neurons developing without synaptic transmission. J Neurosci, 2001. 21(5): p. 1523-31.

38. Tan, E.M., et al., Selective and quickly reversible inactivation of mammalian neurons in vivo using the Drosophila allatostatin receptor. Neuron, 2006. 51(2): p. 157-70.

39. Bhatt, D.H., et al., Grading movement strength by changes in firing intensity versus recruitment of spinal interneurons. Neuron, 2007. 53(1): p. 91-102.

40. Henneman, E., G. Somjen, and D.O. Carpenter, Functional Significance of Cell Size in Spinal Motoneurons. J Neurophysiol, 1965. 28: p. 560-80.
41. Butler, A.B. and W. Hoods, Comparative vertebrate neuroanatomy: evolution and adaptation. 2005, Hoboken, NJ: Wiley-Interscience. 715.
42. Higashijima, S., M. Schaefer, and J.R. Fetcho, Neurotransmitter properties of spinal interneurons in embryonic and larval zebrafish. J Comp Neurol, 2004. 480(1): p. 19-37.
43. Masino, M.A. and J.R. Fetcho, Fictive swimming motor patterns in wild type and mutant larval zebrafish. J Neurophysiol, 2005. 93(6): p. 3177-88.
44. Liu, D.W. and M. Westerfield, Function of identified motoneurones and co-ordination of primary and secondary motor systems during zebra fish swimming. J Physiol, 1988. 403: p. 73-89.
45. Fetcho, J.R., Excitation of motoneurons by the Mauthner axon in goldfish: complexities in a "simple" reticulospinal pathway. J Neurophysiol, 1992. 67(6): p. 1574-86.
46. Fetcho, J.R. and D.S. Faber, Identification of motoneurons and interneurons in the spinal network for escapes initiated by the mauthner cell in goldfish. J Neurosci, 1988. 8(11): p. 4192-213.
47. Crone, S.A., et al., In mice lacking V2a interneurons, gait depends on speed of locomotion. J Neurosci, 2009. 29(21): p. 7098-109.
48. Altman, J. and S.A. Bayer, Development of the brain stem in the rat. IV. Thymidine-radiographic study of the time of origin of neurons in the pontine region. J Comp Neurol, 1980. 194(4): p. 905-29.
49. Lingenhohl, K. and E. Friauf, Giant neurons in the rat reticular formation: a sensorimotor interface in the elementary acoustic startle circuit? J Neurosci, 1994. 14(3 Pt 1): p. 1176-94.

50. Colombo, A., et al., Zebrafish BarH-like genes define discrete neural domains in the early embryo. Gene Expr Patterns, 2006. 6(4): p. 347-52.
51. Moreno, N., et al., LIM-homeodomain genes as territory markers in the brainstem of adult and developing Xenopus laevis. J Comp Neurol, 2005. 485(3): p. 240-54.
52. Passini, M.A., P.A. Raymond, and N. Schechter, Vsx-2, a gene encoding a paired-type homeodomain, is expressed in the retina, hindbrain, and spinal cord during goldfish embryogenesis. Brain Res Dev Brain Res, 1998. 109(2): p. 129-35.
53. Schubert, F.R., et al., Lbx1 marks a subset of interneurons in chick hindbrain and spinal cord. Mech Dev, 2001. 101(1-2): p. 181-5.
54. Storm, R., et al., The bHLH transcription factor Olig3 marks the dorsal neuroepithelium of the hindbrain and is essential for the development of brainstem nuclei. Development, 2009. 136(2): p. 295-305.
55. Thaeron, C., et al., Zebrafish evx1 is dynamically expressed during embryogenesis in subsets of interneurones, posterior gut and urogenital system. Mech Dev, 2000. 99(1-2): p. 167-72.
56. Drapeau, P., et al., In vivo recording from identifiable neurons of the locomotor network in the developing zebrafish. J Neurosci Methods, 1999. 88(1): p. 1-13.